Concrete Systems for a 100-Year Design Life

Final Report
2025

Principal Investigator: Dr. Eric Landis

Authors:
Eric Landis
Erfan Najaf

Sponsored By
Transportation Infrastructure Durability Center
List other Sponsors if applicable (i.e. MaineDOT)

TIDC

Transportation Infrastructure Durability Center
AT THE UNIVERSITY OF MAINE

A report from
University of Maine

THE UNIVERSITY OF MAINE 1865 | UMASS LOWELL | WESTERN NEW ENGLAND UNIVERSITY WNE | UCONN | THE UNIVERSITY OF RHODE ISLAND | The UNIVERSITY of VERMONT

About the Transportation Infrastructure Durability Center

The Transportation Infrastructure Durability Center (TIDC) is the 2018 US DOT Region 1 (New England) University Transportation Center (UTC) located at the University of Maine Advanced Structures and Composites Center. TIDC's research focuses on efforts to improve the durability and extend the life of transportation infrastructure in New England and beyond through an integrated collaboration of universities, state DOTs, and industry. The TIDC is comprised of six New England universities, the University of Maine (lead), the University of Connecticut, the University of Massachusetts Lowell, the University of Rhode Island, the University of Vermont, and Western New England University.

U.S. Department of Transportation (US DOT) Disclaimer

Acknowledgements

Funding for this research is provided by the Transportation Infrastructure Durability Center at the University of Maine under grant 69A3551847101 from the U.S. Department of Transportation's University Transportation Centers Program. [Include any acknowledgements for other contributors (i.e. your university or contributing DOTs/industry partners) here.]

1. Report No.	2. Government Accession No.	3. Recipient Catalog No.
4 Title and Subtitle Concrete Systems for a 100-Year Design Life		5 Report Date 6 Performing Organization Code
7. Author(s) Erfan Najaf https://orcid.org/0000-0001-7953-2947 Eric Landis https://orcid.org/0000-0003-4934-9150		8 Performing Organization Report No.
9 Performing Organization Name and Address Transportation Infrastructure Durability Center		10 Work Unit No. (TRAIS) 11 Contract or Grant No.
12 Sponsoring Agency Name and Address		13 Type of Report and Period Covered 14 Sponsoring Agency Code
15 Supplementary Notes		

16 Abstract

Early-age cracking, driven by shrinkage and thermal stresses, is a critical durability concern for concrete infrastructure, particularly in the cold climates of the New England region. This report presents a comprehensive, three-pronged investigation into developing practical and sustainable strategies to produce more crack-resistant concrete. The research integrates fundamental mix design optimization, full-scale structural analysis, and the use of advanced nanomaterials.

The first phase focused on creating an inherently low-shrinkage and sustainable concrete mix. By optimizing aggregate gradation using the Tarantula Curve methodology, the cement content was significantly reduced. This approach paradoxically increased the 28-day flexural strength by up to 49% while simultaneously reducing drying shrinkage by over 25% and CO_2 emissions by 30%. The incorporation of 15% pre-wetted lightweight fine aggregate (LWFA) for internal curing provided an additional 20% reduction in shrinkage with only a minor trade-off in mechanical strength.

The second phase quantified the risk of thermal cracking in composite bridge decks. An analysis of in-situ temperature data from a concrete-on-steel-girder bridge revealed that thermal gradients, driven by the heat of hydration and ambient temperature swings, can induce tensile strains that exceed the concrete's early-age capacity, leading to cracking. A computational model demonstrated that controlling the temperature differential between the concrete and steel to within 4-5°C is an effective strategy to mitigate this risk.

<table>
<tr><td colspan="4">The third phase evaluated the potential of Cellulose Nanofibrils (CNF) as a performance-enhancing admixture. The results showed that an optimal dosage of 0.3% CNF by weight of cement increased 28-day flexural strength by 28%, reduced drying shrinkage by 17%, and improved durability by increasing bulk resistivity by over 20%.
Collectively, this research demonstrates that a holistic approach—combining an optimized, low-cement mix design with internal curing, implementing thermal controls during construction, and leveraging advanced admixtures like CNF—provides a robust and effective pathway to minimize cracking and significantly enhance the durability and service life of transportation infrastructure.</td></tr>
<tr><td colspan="2">17 Key Words
• Early-Age Cracking
• Shrinkage
• Thermal Stress
• Mix Design Optimization
• Aggregate Gradation
• Cement Reduction
• Internal Curing
• Cellulose Nanofibrils (CNF)
• Sustainability
•</td><td colspan="2">18 Distribution Statement
No restrictions. This document is available to the public through</td></tr>
<tr><td>19 Security Classification (of this report)
Unclassified</td><td>20 Security Classification (of this page)
Unclassified</td><td>21 No. of pages</td><td>22 Price</td></tr>
</table>

Technical Report Documentation Page

Form DOT F 1700.7 (8-72)

Contents

List of Figures

List of Tables

List of Key Terms

- **Aggregate Gradation:** The distribution and proportion of different particle sizes within a collection of aggregates. Optimized gradation aims to minimize void space and reduce the required amount of cement paste.

- **ASTM:** American Society for Testing and Materials. The organization that develops and publishes voluntary consensus technical standards for a wide range of materials, products, systems, and services.

- **Autogenous Shrinkage:** The volumetric reduction of concrete due to the chemical process of cement hydration, which consumes water from the mix. It occurs without any loss of moisture to the environment.

- **Bulk Resistivity:** An intrinsic property of concrete that measures its resistance to the flow of electrical current. It is used as a key indicator of the concrete's permeability and potential durability, with higher values indicating a denser, less permeable microstructure.

- **Cement-to-Aggregate (C/A) Ratio:** The ratio, typically by weight, of the total cementitious material to the total aggregate in a concrete mix.

- **Cellulose Nanofibrils (CNF):** A renewable, bio-based nanomaterial derived from wood pulp. In this study, it is used as an admixture to provide micro-reinforcement and enhance shrinkage resistance in concrete.

- **Composite Bridge Deck:** A type of bridge construction where the concrete deck and steel support girders are structurally connected to act as a single, unified unit, enhancing stiffness and load-carrying capacity.

- **Drying Shrinkage:** The volumetric reduction of hardened concrete caused by the loss of moisture to the surrounding environment.

- **Flexural Strength (Modulus of Rupture):** A measure of a material's ability to resist failure under bending loads. It is a critical property for predicting the cracking resistance of concrete beams and slabs.

- **Internal Curing:** A technique that provides a localized source of water within the concrete matrix during hydration to mitigate self-desiccation and autogenous shrinkage. In this study, it is achieved using pre-wetted lightweight fine aggregates.

- **Life Cycle Assessment (LCA):** A methodology for evaluating the environmental impacts associated with all stages of a product's life, from raw material extraction through processing, manufacturing, use, and disposal or recycling.

- **Lightweight Fine Aggregate (LWFA):** A porous, low-density aggregate that can absorb and later release water, making it an effective agent for internal curing.

- **Portland Limestone Cement (PLC):** A type of blended cement that contains a higher percentage of interground limestone than ordinary portland cement, resulting in a lower carbon footprint.

- **Tarantula Curve:** A specific graphical tool and methodology used to optimize the combined gradation of aggregates in a concrete mix to improve packing density, workability, and overall performance.

- **Thermal Gradient:** The rate of temperature change over a distance. In this report, it refers specifically to the difference in temperature between the concrete deck and the supporting steel structure, which induces stress.

Abstract:

Early-age cracking, driven by shrinkage and thermal stresses, is a critical durability concern for concrete infrastructure, particularly in the cold climates of the New England region. This

report presents a comprehensive, three-pronged investigation into developing practical and sustainable strategies to produce more crack-resistant concrete. The research integrates fundamental mix design optimization, full-scale structural analysis, and the use of advanced nanomaterials.

The first phase focused on creating an inherently low-shrinkage and sustainable concrete mix. By optimizing aggregate gradation using the Tarantula Curve methodology, the cement content was significantly reduced. This approach paradoxically increased the 28-day flexural strength by up to 49% while simultaneously reducing drying shrinkage by over 25% and CO_2 emissions by 30%. The incorporation of 15% pre-wetted lightweight fine aggregate (LWFA) for internal curing provided an additional 20% reduction in shrinkage with only a minor trade-off in mechanical strength.

The second phase quantified the risk of thermal cracking in composite bridge decks. An analysis of in-situ temperature data from a concrete-on-steel-girder bridge revealed that thermal gradients, driven by the heat of hydration and ambient temperature swings, can induce tensile strains that exceed the concrete's early-age capacity, leading to cracking. A computational model demonstrated that controlling the temperature differential between the concrete and steel to within 4-5°C is an effective strategy to mitigate this risk.

The third phase evaluated the potential of Cellulose Nanofibrils (CNF) as a performance-enhancing admixture. The results showed that an optimal dosage of 0.3% CNF by weight of cement increased 28-day flexural strength by 28%, reduced drying shrinkage by 17%, and improved durability by increasing bulk resistivity by over 20%.

Collectively, this research demonstrates that a holistic approach—combining an optimized, low-cement mix design with internal curing, implementing thermal controls during construction, and leveraging advanced admixtures like CNF—provides a robust and effective pathway to minimize cracking and significantly enhance the durability and service life of transportation infrastructure.

Chapter 1:Introduction and Background

The long-term durability of concrete infrastructure is a cornerstone of a functional and safe transportation network. However, in regions with demanding freeze-thaw cycles and aggressive environmental conditions, such as the American Northeast, the service life of concrete structures is often compromised by premature deterioration. A primary contributor to this issue is early-age cracking, a phenomenon driven by volumetric changes in the concrete, specifically autogenous and drying shrinkage. These initial cracks, while small, create pathways for water and de-icing salts to penetrate the concrete, accelerating reinforcement corrosion and leading to costly repairs and reduced structural longevity. The challenge is particularly acute in composite structures like steel-girder bridges, where the concrete deck is restrained by the steel beams, leading to significant thermal stresses that exacerbate the risk of cracking, especially during cold-weather construction.

Addressing this multifaceted problem requires a comprehensive approach that looks beyond a single solution. A truly durable concrete is not only resistant to cracking but is also sustainable and practical for real-world application. This project was therefore motivated by the need to develop a holistic set of strategies to mitigate shrinkage and cracking in concrete from three distinct but interconnected perspectives: fundamental material design, structural-level thermal analysis, and the integration of advanced material additives.

First, the project is motivated by the need to create a more inherently stable and sustainable concrete mix from the ground up. Conventional concrete mixes often rely on high cement content, which increases cost, carbon footprint, heat of hydration, and susceptibility to shrinkage. This motivated the first phase of the project: to systematically optimize concrete mix designs by improving aggregate gradation using methodologies like the Tarantula Curve. By enhancing particle packing, the volume of cement paste can be reduced, which in turn lowers shrinkage. This phase also explores the use of internal curing agents, such as pre-wetted lightweight fine aggregates (LWFA), to provide a localized water source that counteracts self-desiccation and drying shrinkage from within the concrete matrix.

Second, the project is motivated by the critical need to understand and control the real-world stresses that occur in bridge structures during their most vulnerable early stages. Even an optimized concrete mix can crack if subjected to extreme thermal gradients. The differential

thermal properties of concrete and steel mean that as the concrete cures and cools, significant tensile stresses develop in the deck. This motivated the second phase of the project: to analyze temperature data from an active bridge to quantify these thermal strains and model their impact on the concrete. This analysis provides the basis for exploring practical mitigation strategies, such as the application of external heating, to reduce the temperature difference between the concrete deck and steel girders, thereby minimizing the risk of thermal cracking.

Finally, the project is motivated by the potential of advanced materials to provide an additional layer of defense against cracking at the microstructural level. This led to the third phase of the project, which investigates the use of Cellulose Nanofibrils (CNF) as a novel concrete additive. The motivation here is to determine if these nanoscale fibers can act as micro-reinforcement, bridging microcracks as they initiate, refining the pore structure, and enhancing internal curing. By improving both the mechanical properties (compressive and flexural strength) and the shrinkage resistance of the concrete, CNF offers a promising pathway to further enhance durability.

In summary, this project undertakes a multi-scale investigation—from the optimization of constituent materials and the integration of advanced additives to the analysis of full-scale structural behavior—to develop a robust and integrated set of solutions for producing more durable, crack-resistant, and sustainable concrete for critical transportation infrastructure.

1-1- Literature review

Minimizing shrinkage in concrete involves optimizing aggregate grading and reducing cement content. Research suggests that increasing the proportion of aggregates can effectively lower shrinkage, enhance material properties, reduce production costs, and decrease carbon dioxide emissions [1]. A high cement content often results in unstable mixes, increased drying and autogenous shrinkage, elevated heat of hydration, and a greater likelihood of cracking, emphasizing the necessity of optimizing cement levels [2]. Aggregate grading is crucial for concrete performance, as studies indicate that refining the granular skeleton enhances aggregate structure compactness, leading to improved concrete properties regardless of variations in aggregate shape, size, or composition [3]. The application of

Fuller's grading curve in numerical simulations has demonstrated its effectiveness in optimizing concrete compactness and strength, reinforcing the importance of aggregate grading [4]. Structuring aggregate particle sizes to achieve optimal gradation and compactness is recognized as a beneficial approach to improving concrete properties [5]. The composition of concrete mixtures plays a significant role in shrinkage and performance. Comparisons between concrete made with mined and crushed aggregates reveal that mined aggregates tend to result in lower shrinkage, highlighting the impact of aggregate composition on material behavior [6]. Additionally, increasing the utilization of crushed natural and recycled fine aggregates contributes to resource conservation and waste recycling in construction [7]. The use of crushed clinker brick waste as coarse aggregate has been shown to enhance concrete compressive strength by refining the gradation curve, demonstrating the significance of sustainable aggregate choices [8]. Packing density of aggregates and cement content are critical factors influencing concrete mixture design, affecting strength, durability, elastic modulus, and creep behavior [9]. By optimizing mixtures for higher packing density and lower cement content, improved performance can be achieved. The evaluation of fine aggregates for mortar and concrete applications is essential in ensuring desired properties [10]. The combined gradation of coarse aggregates influences both compressive strength and workability, demonstrating that variations in aggregate sizes impact concrete performance [11]. Predicting voids in coarse aggregates is a fundamental aspect of designing stone matrix asphalt mixtures, underscoring the significance of aggregate gradation in asphalt concrete performance [12]. Adjusting particle sizes in recycled-aggregate concrete helps mitigate defects associated with recycled aggregates, emphasizing the need to optimize aggregate properties for sustainable concrete production [13].

The relationship between aggregate volume and concrete shrinkage is a critical research area due to its implications for the durability and performance of concrete structures. Increasing the aggregate volume in concrete mixes has been shown to significantly reduce shrinkage. This reduction occurs due to two main mechanisms: first, by decreasing the shrinkage component within the cement paste matrix, and second, by providing a skeletal structure that counteracts overall shrinkage [41]. Aggregates not only dilute shrinkage effects within the cement paste but also enhance concrete’s mechanical properties, improving dimensional

stability [42]. Another key aspect of concrete mix optimization is aggregate grading. The Tarantula curve, is a graphical tool used to optimize aggregate proportions, improving workability and reducing cement paste content [43]. This method has been widely implemented by various state Departments of Transportation (DOTs) in the United States, highlighting its practical relevance in concrete engineering [44]. Following the principles of the Tarantula curve enables more efficient aggregate packing, which minimizes voids and enhances overall concrete performance [45]. Research has confirmed that aggregate size and gradation influence drying shrinkage. For example, Maruyama and Sugie [46] conducted a numerical study showing a trade-off between concrete flowability and shrinkage, suggesting that selecting an optimal aggregate size can mitigate shrinkage while maintaining workability [47]. Studies also show that larger aggregate sizes contribute to lower shrinkage, as they provide greater resistance against shrinkage within the cement paste [48]. This effect is particularly pronounced in self-compacting concretes (SCCs), where the volume and gradation of coarse aggregates are key factors in controlling drying shrinkage [49]. Furthermore, the physical properties of aggregates, such as water absorption, play a crucial role in shrinkage behavior. Yagi et al. [41] found that aggregate volume changes are closely linked to water absorption capacity, which directly affects drying shrinkage [50]. This relationship highlights the importance of selecting aggregates with appropriate absorption characteristics to minimize shrinkage and improve durability [51]. Research by Hua et al. [44] suggests that recycled aggregates can be successfully incorporated into concrete mixes, though further experimentation is necessary to fully assess their impact on shrinkage and overall performance [42]. While recycled aggregates promote sustainability, they introduce challenges related to shrinkage control, as their properties can vary significantly [52].

Internal curing techniques help mitigate shrinkage by maintaining adequate moisture levels during hydration. This method involves incorporating materials such as pre-wetted lightweight aggregates or super absorbent polymers into the mix to serve as internal water reservoirs, gradually releasing moisture [14]. By enhancing internal humidity through controlled water release, cement hydration is sustained, reducing self-desiccation and improving overall concrete performance [15]. Internal curing is particularly valuable in high-performance concrete (HPC), where it minimizes autogenous shrinkage and reduces early-age cracking [16,17]. Studies indicate that internal curing using pre-soaked lightweight

aggregates (PS-LWA) positively affects shrinkage control and interior relative humidity, leading to improved compressive strength [18]. Although lightweight aggregates may slightly reduce strength, their ability to facilitate internal curing effectively mitigates autogenous shrinkage and cracking [19]. These aggregates act as moisture reservoirs, absorbing and gradually releasing water to counteract shrinkage, making them essential in lightweight structural concrete applications [20]. In bridge decks, combining internal curing with supplementary cementitious materials (SCMs) and pre-wetted fine lightweight aggregates has been shown to produce high-performance, low-shrinkage concrete, minimizing cracking [21]. Furthermore, shrinkage-reducing admixtures (SRAs) are widely recognized for their effectiveness in reducing shrinkage and preventing cracks [22]. Internal curing has also been shown to improve compressive strength while reducing autogenous shrinkage, leading to enhanced concrete properties [23]. Several studies confirm that using lightweight aggregates for internal curing decreases shrinkage and improves concrete durability [24]. Additional advantages of lightweight aggregate concrete include reductions in early-age shrinkage, decreased dead loads, resulting in cost savings on foundations and reinforcement, and enhanced thermal insulation [25]. Partial substitution of natural sand with lightweight pumice aggregate further reduces both drying and autogenous shrinkage while enhancing mechanical properties [26]. Other internal curing agents, such as crushed clay bricks or lightweight aggregates, have proven effective in reducing autogenous shrinkage and enhancing concrete performance [27]. Lightweight aggregates facilitate water transport within the concrete matrix, supporting the internal curing process [28]. Additionally, incorporating materials such as porcelanite has been found to increase compressive strength due to internal curing, particularly with prolonged curing periods [29].

In addition, reducing cement content has been recognized as one of the most effective strategies for minimizing carbon emissions in concrete production. The cement manufacturing process is a major contributor to carbon emissions, making it a critical target for reduction initiatives [30]. Lowering the cement content in concrete mixes significantly reduces embodied carbon emissions [31]. Research has explored alternative materials to partially replace cement, such as waste ceramic powder, which provides a sustainable solution [32]. Utilizing ceramic waste powder and rice husk ash as partial cement substitutes not only lowers the carbon footprint but also promotes efficient waste utilization [33]. The

use of mineral admixtures like metakaolin has also been identified as an effective method for reducing cement content while mitigating environmental impact [34]. Similarly, incorporating fly ash as a cement replacement improves concrete performance while reducing emissions [35]. Innovative approaches, such as using biomass fly ash in geopolymeric materials, further contribute to emission reductions [36]. Geopolymer technology provides a sustainable alternative by utilizing industrial byproducts. Other waste materials, including eggshell ash and palm oil fuel ash, have demonstrated potential for reducing concrete's environmental footprint [37]. Optimizing concrete mix designs to decrease cement consumption and associated emissions is another viable strategy. Studies suggest that replacing portions of cement with stone powder reduces cement consumption while maintaining compressive strength [38]. The use of superplasticizers improves workability and optimizes cement particle distribution in water, leading to a more complete hydration process and potential cement reduction [39]. In conclusion, a combination of alternative materials, optimized mix designs, and chemical admixtures supports sustainable concrete production, minimizing environmental impact and promoting resource efficiency.

1-2- Research, Objectives, and Tasks

The overarching goal of this research is to develop and validate a multi-pronged approach to minimize early-age cracking in concrete for transportation infrastructure. This goal is broken down into three primary objectives, each with a corresponding set of research tasks.

Objective 1: Develop a sustainable, low-shrinkage concrete through fundamental mix design optimization.

- **Task 1.1:** Analyze and optimize the combined aggregate gradation of standard concrete mixes using the Tarantula Curve methodology to enhance packing density.
- **Task 1.2:** Systematically reduce the cement-to-aggregate ratio and evaluate the effects on workability, mechanical properties (compressive and flexural strength), shrinkage, and durability (bulk resistivity).
- **Task 1.3:** Incorporate pre-wetted lightweight fine aggregates (LWFA) at various replacement levels (5%, 10%, 15%) to assess their effectiveness as an internal curing agent for shrinkage mitigation.

- **Task 1.4:** Conduct a Life Cycle Assessment (LCA) to quantify the environmental benefits, particularly the reduction in CO_2 emissions, of the optimized mix designs.

Objective 2: Analyze and mitigate thermal stress in composite bridge decks during early-age curing.

- **Task 2.1:** Collect and analyze real-world temperature data from the concrete deck and steel girders of a composite bridge to quantify in-situ thermal gradients.
- **Task 2.2:** Develop a computational model using MATLAB to calculate the time-dependent development of thermal strains and stresses in the concrete deck based on the measured temperature differential.
- **Task 2.3:** Compare the calculated total strain (thermal + shrinkage) against the concrete's allowable tensile strain capacity to predict the risk of cracking.
- **Task 2.4:** Model and evaluate various mitigation scenarios, such as applying external heat, to determine the required reduction in the temperature differential to prevent thermal cracking.

Objective 3: Evaluate the efficacy of Cellulose Nanofibrils (CNF) as a performance-enhancing admixture.

- **Task 3.1:** Prepare concrete specimens with varying dosages of CNF (ranging up to 0.3% and higher by weight of cement).
- **Task 3.2:** Conduct mechanical property tests (28-day compressive and flexural strength) to determine the optimal CNF dosage for strength enhancement.
- **Task 3.3:** Perform shrinkage tests (ASTM C157) on CNF-modified concrete specimens to quantify the impact of CNF on shrinkage reduction over 28 days.

1-3- Report Overview

This report documents the comprehensive investigation into mitigating shrinkage and cracking in concrete through three interconnected research phases. The structure of the report is designed to present the methodology, results, and conclusions of each phase in a clear and logical sequence, culminating in a set of integrated recommendations.

- **Chapter 1** provides the introduction, background, and motivation for the project, outlines the specific research objectives and tasks, and presents this overview of the report's structure.
- **Chapter 2** details the experimental program and methodologies employed across all three research phases. This includes descriptions of the materials used, the concrete mix designs, the specimen preparation procedures, and the standardized testing protocols for mechanical properties, shrinkage, and durability.
- **Chapter 3** presents the results and discussion for the first research phase: the development of low-shrinkage concrete through aggregate optimization, cement reduction, and internal curing with LWFA.
- **Chapter 4** presents the results and discussion for the second research phase: the thermal analysis of a composite bridge deck. This chapter details the temperature data, the MATLAB modeling of thermal strains, and the evaluation of mitigation scenarios.
- **Chapter 5** presents the results and discussion for the third research phase: the evaluation of Cellulose Nanofibrils (CNF) as a shrinkage-reducing admixture.
- **Chapter 6** provides the overall conclusions drawn from the integrated findings of the three research phases. It synthesizes the key results and offers a set of comprehensive recommendations for designing and constructing durable, sustainable, and crack-resistant concrete infrastructure.

Chapter 2: Methodology

This chapter details the materials, experimental procedures, and analytical methods used across the three interconnected phases of this research project. The methodology is organized to first describe the constituent materials common to the project, followed by the specific test setups and processes for each research objective: (1) mix design optimization, (2) thermal strain analysis, and (3) evaluation of Cellulose Nanofibrils (CNF).

2-1- Materials

2-1-1- Cementitious Materials

Two primary types of cementitious materials were used in this study: Portland Cement and Slag. For the initial baseline mix, **PORTLAND CEMENT-TYPE II** was used. For all subsequent optimized mixes, **PORTLAND LIMESTONE CEMENT (PLC)** was used to improve sustainability and performance. **SLAG, GRADE 120** was used as a supplementary cementitious material in a 50/50 replacement ratio with the cement by weight. The chemical properties of these materials, determined in accordance with ASTM C114-18, are provided in Table 1.

Table 1.Chemical properties of PLC, Cement and Slag

Oxides	PLC (%)	Cement (%)	Slag (Grade 120,) (%)
SiO_2	20.2	21.5	32.70
Al_2O_3	3.6	3.7	8.58
Fe_2O_3	3.2	3.3	1.70
CaO	65.1	65.2	44.82
MgO	3.0	3.4	9.33
SO_3	3.4	3.3	1.16
Na_2O	0.3	--	0.30

2-1-2- Aggregates and Gradation Optimization

The aggregate blend was a critical focus of this study. The initial reference mix was based on the standard Maine DOT Class A concrete, which has a coarse-to-fine aggregate ratio of

68:32. This gradation, however, does not fall within the optimal boundaries of the Tarantula Curve.

To improve particle packing density and reduce paste content, the aggregate gradation was optimized using the **Tarantula Curve** methodology. The ratio was adjusted to **55% coarse aggregate and 45% fine aggregate**, and the 3/8" coarse aggregate was excluded to ensure the blend remained within the curve's specified limits. This optimized gradation complies with ASTM C33M-18 standards. The water absorption rates were 1.24% for fine aggregate and 0.94% for coarse aggregate. The figures below illustrate the gradation analysis.

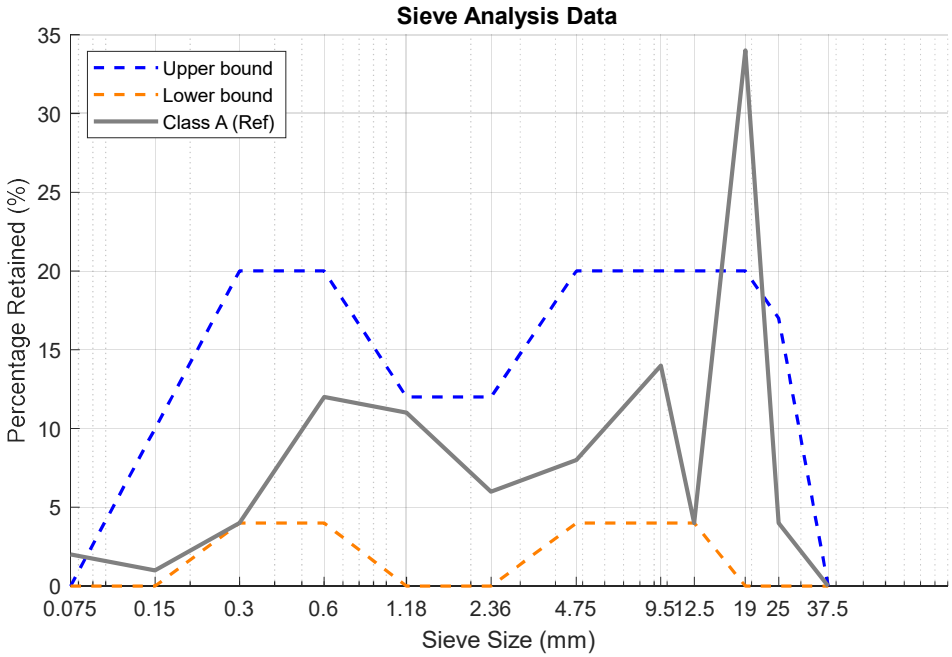

Figure 1a. Aggregate grading for the standard Maine DOT mix design, showing its position outside the Tarantula Curve bounds.

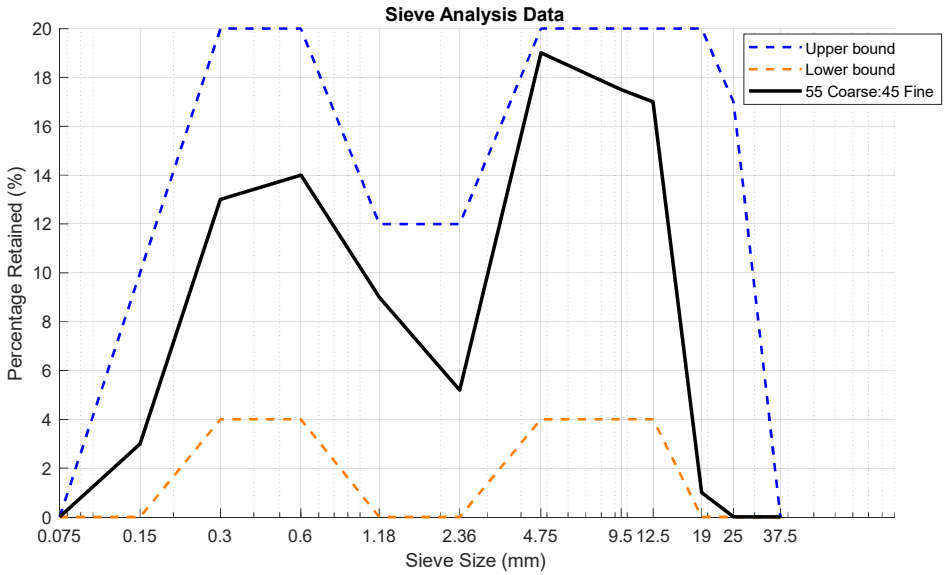

Figure 1c. Aggregate grading for the optimized 55:45 mix, showing compliance with the Tarantula Curve.

2-1-3- Lightweight Aggregate (LWA) for Internal Curing

For the internal curing portion of the study, **Norlite lightweight aggregate (LWA)** was used as a partial replacement for fine aggregate. Its low density and high porosity make it an effective internal reservoir for water, which is gradually released during hydration to mitigate autogenous shrinkage. LWA was incorporated at replacement levels of 5%, 10%, and 15% by weight of the fine aggregate. The gradations for these LWA-modified mixes were also verified to be within the Tarantula Curve limits.

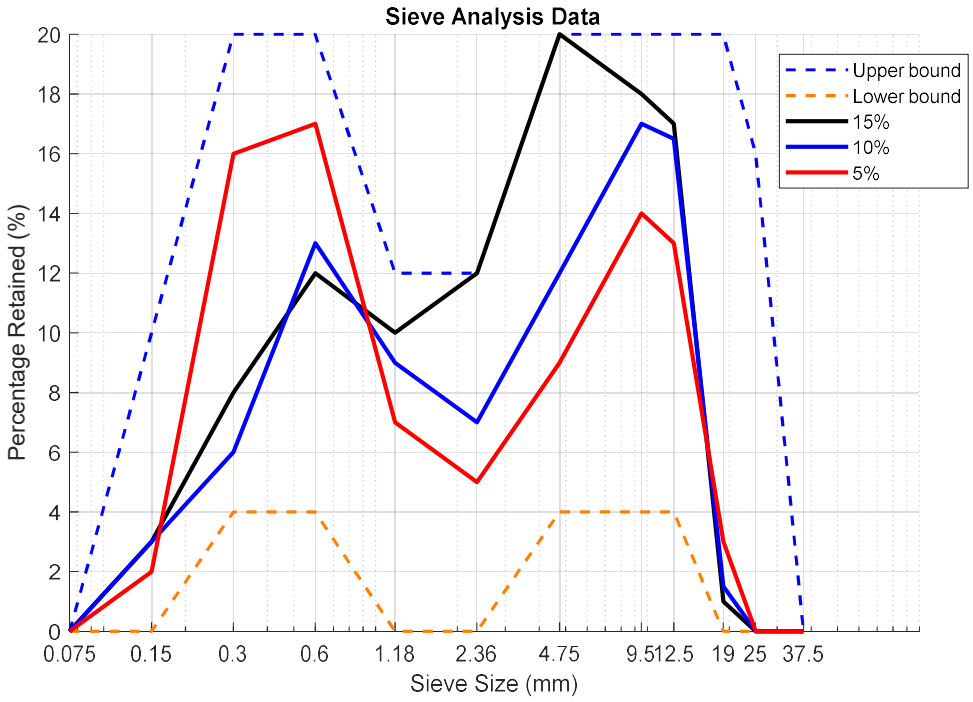

Figure 1c. Gradation curves for lightweight aggregate (LWA) mixes (5%, 10%, 15%), confirming all are within the Tarantula Curve limits.

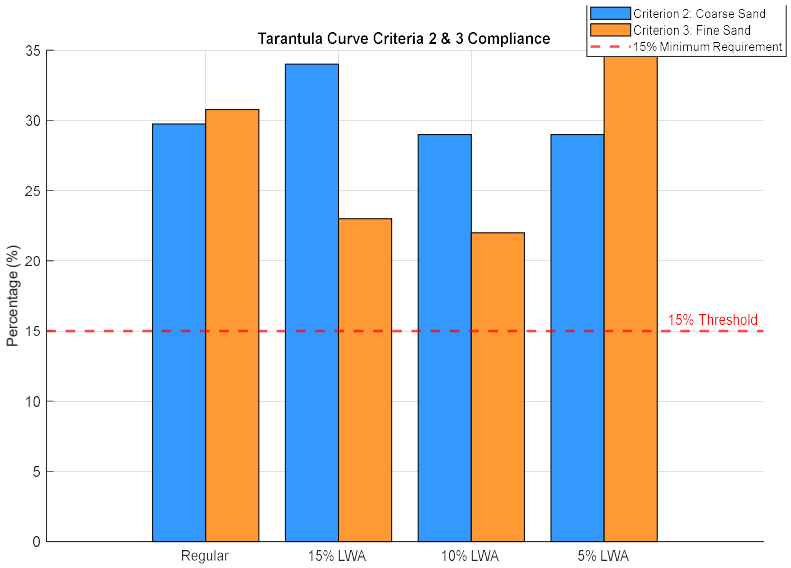

Figure 1d. Compliance of regular and LWA-modified mixes with Tarantula Curve Criterion 2 (Coarse Sand) and Criterion 3 (Fine Sand).

2-1-4- Chemical Admixtures

To maintain workability, especially in mixes with reduced cement paste content, a high-range water reducer (HRWR) was used. The superplasticizer was **MASTERGLENIUM 7500**, a polycarboxylate-based admixture compliant with ASTM C494 and C1017. An air-entraining admixture (AE) was also used.

2-1-5- Cellulose Nanofibrils (CNF)

For the third phase of the study, **Cellulose Nanofibrils (CNF)** were introduced as a performance-enhancing admixture. The CNF was added to a baseline Maine DOT "Class A" 30 MPa concrete mix at various dosages to evaluate its effect on mechanical properties and shrinkage resistance.

2-2- Test Setup & Process

2-2-1- Phase 1: Concrete Mixing, Specimen Preparation, and Testing

A series of concrete mixes were designed to evaluate the effects of reducing the cement-to-aggregate (C/A) ratio and incorporating LWA. The comprehensive list of mix designs is detailed in Table 2.

Table 2.Mix design proportions for concrete specimens (per yd³)

Mix Design	Cement to Aggregate ratio	Cement (lb/yd3)	Slag (lb/yd3)	Water (lb/yd3)	Coarse (lb/yd3)	Fine (lb/yd3)	LWA (lb/yd3)	HRWR (oz/yd3)	AE (oz/yd3)	Type
1	0.21	320	320	244	1639	1341	0	25.6	1.92	Regular
2	0.18	268	268	241.5	1639	1341	0	38.4	1.92	Regular
3	0.165	246	246	221.4	1639	1341	0	51.2	1.92	Regular
4	0.15	224	224	201.5	1639	1341	0	76.8	1.92	Regular
5	0.15	224	224	201.5	1490	1490	0	76.8	1.92	Regular
6	0.21	320	320	244	1639	894	447	25.6	1.92	LWC (15%)
7	0.18	268	268	241.5	1639	894	447	30.72	1.92	LWC (15%)
8	0.165	246	246	221.4	1639	894	447	38.4	1.92	LWC (15%)
9	0.15	224	224	201.5	1639	894	447	43.52	1.92	LWC (15%)
10	0.21	320	320	244	1639	2682	298	23.04	1.92	LWC (10%)
11	0.18	268	268	241.5	1639	2682	298	32.64	1.92	LWC (10%)

12	0.165	246	246	221.4	1639	2682	298	41.28	1.92	LWC (10%)
13	0.15	224	224	201.5	1639	2682	298	46.08	1.92	LWC (10%)
14	0.21	320	320	244	1639	2831	149	20.48	1.92	LWC (5%)
15	0.18	268	268	241.5	1639	2831	149	28.8	1.92	LWC (5%)
16	0.165	246	246	221.4	1639	2831	149	36.48	1.92	LWC (5%)
17	0.15	224	224	201.5	1639	2831	149	41.6	1.92	LWC (5%)

Mixing and Curing: For all mixes, ingredients were added to a drum mixer. For mixes containing LWA, the LWA was pre-soaked for 24 hours and drained to a saturated surface-dry (SSD) condition before mixing. Freshly mixed concrete was tested for slump (ASTM C143). Specimens were cast in molds, kept in a controlled environment (23 ± 2 °C, ≥95% RH) for 24 hours, and then demolded and transferred to a wet curing room until the designated testing age.

Testing Procedures: A series of standardized tests were performed to evaluate the concrete properties, as summarized in Table 3.

Table 3. Testing matrix for concrete specimens

	Shrinkage Measurement	Compression Test	Flexure Test	Bulk Resistivity Measurement
Quantity	3	3	3	3
ASTM standards	C157	C39	C78	C1876

2-2-2- Phase 2: Thermal Strain Analysis of Composite Bridge Deck

This phase involved a computational analysis to model the thermal behavior of a concrete bridge deck on steel girders.

1. **Data Acquisition:** Temperature data was collected from an in-service bridge, recording the temperature profiles of both the concrete deck and the supporting steel beams over time.
2. **Material Property Modeling:** The time-dependent development of key concrete properties was modeled in MATLAB using established equations:
    - **Compressive Strength (**fc(t)**):** Calculated using the ACI 209 (2008) model.
    - **Modulus of Elasticity (**Ec(t)**):** Calculated using the ACI 318 (2019) model.

- **Tensile Strength (**ft(t)**):** Calculated using the relationship proposed by Raphael (1984).

3. **Thermal Strain Calculation:** The thermal strain (ϵT) resulting from the temperature differential (ΔT) between the concrete and steel was calculated. The total strain was determined by adding the calculated shrinkage strain to the thermal strain.
4. **Cracking Risk Analysis:** The calculated total strain in the concrete was compared to its allowable tensile strain capacity (derived from its tensile strength and modulus of elasticity) to assess the risk of cracking over time. Various scenarios reducing the temperature differential were modeled to evaluate the effectiveness of mitigation strategies like external heating.

2-2-3- Phase 3: Evaluation of CNF

The methodology for this phase focused on determining the influence of CNF on a standard concrete mix.

1. **Specimen Preparation:** A Maine DOT "Class A" concrete mix was used as the control. Additional batches were prepared with varying CNF dosages (e.g., 0.1%, 0.2%, 0.3% by weight of cement).
2. **Testing:** The CNF-modified specimens were subjected to the same standardized tests as in Phase 1 to evaluate their performance relative to the control mix:
    - Compressive Strength (ASTM C39) at 28 days.
    - Flexural Strength (ASTM C78) at 28 days.
    - Drying Shrinkage (ASTM C157) monitored for 28 days.

Chapter 3: Results and Discussion: Mix Design Optimization for Durability and Sustainability

This chapter presents the results from the first phase of the research, which focused on developing a sustainable, low-shrinkage concrete by optimizing the fundamental mix design. The investigation centered on two primary strategies: (1) reducing the cement paste volume through optimized aggregate gradation, and (2) mitigating shrinkage through the use of internal curing with pre-wetted lightweight fine aggregates (LWFA). The following sections detail the effects of these strategies on the concrete's fresh properties, mechanical performance, durability potential, and environmental impact.

3-1- Performance of Optimized Regular Concrete

This section evaluates the performance of concrete mixes without LWA, where the primary variable was the cement-to-aggregate (C/A) ratio. The goal was to determine the extent to which cement content could be reduced while maintaining or improving performance.

3-1-1- Workability and Fresh Properties

A critical initial assessment was the workability of the concrete, measured by the slump test (ASTM C143). As the volume of cement paste was reduced, a corresponding decrease in workability was anticipated. The results, summarized in Table 4, confirm this trend.

Table 4. Compressive strength and slump test results for regular concrete

NO.	Name	7 days (MPa)	14 days (MPa)	28 days (MPa)	Slump (mm)
1	0.21 (Type II)	18.29	22.59	28.29	132
2	0.21 (PLC)	18.99	25.09	30.19	139
3	0.18 (PLC)	24.09	31.19	37.59	127
4	0.165 (PLC)	27.39	35.29	42.19	114
5	0.15a (PLC)	24.49	31.69	37.39	73
6	0.15b (PLC)	23.19	29.89	39.70	89

The baseline mixes with a C/A ratio of 0.21 exhibited high slump values (132-139 mm), indicating excellent workability. As the C/A ratio was reduced to 0.18 and 0.165, the slump decreased but remained in a highly workable range (127 mm and 114 mm, respectively). However, the mix with a C/A ratio of 0.15 (Mix 5, 0.15a) showed a significant drop in slump to 73 mm, indicating a stiff, challenging mix. This is because the reduced paste volume was insufficient to effectively lubricate the aggregate particles in the 55:45 coarse-to-fine aggregate blend. To counteract this, the aggregate proportion was adjusted to a more balanced 50:50 ratio (Mix 6, 0.15b), which successfully improved the slump to 89 mm. This demonstrates a critical interplay between paste volume and aggregate gradation in controlling the fresh properties of concrete.

3-1-2- Compressive Strength Development

The compressive strength of the concrete was tested at 7, 14, and 28 days. The results, shown in Figure 2 and detailed in Table 4 above, reveal a compelling trend: reducing the cement content, when paired with an optimized aggregate skeleton, significantly increases compressive strength.

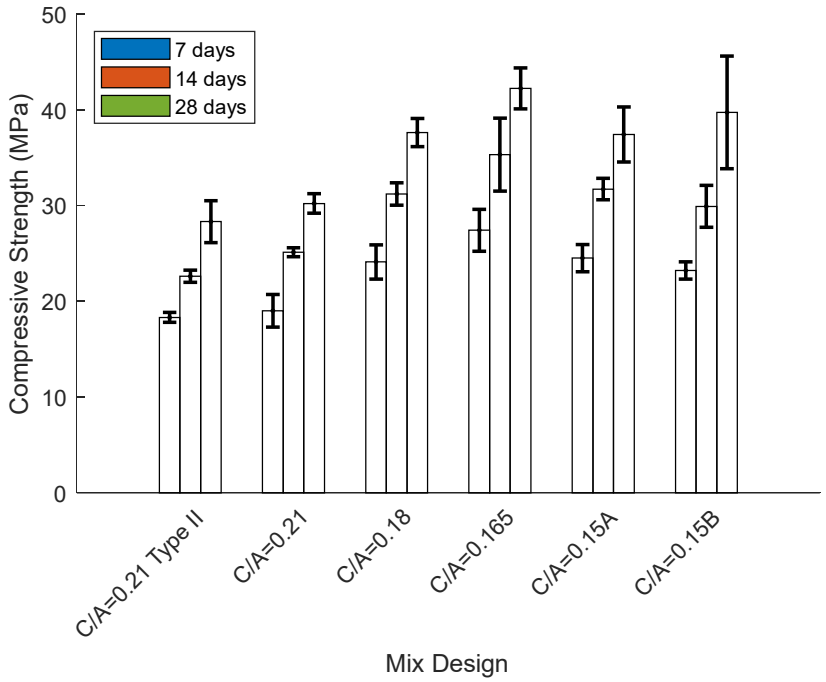

Figure 2.Comparison of compressive strength development for regular concrete mixes.

The reference mix using Type II cement (Mix 1) reached a 28-day strength of 28.3 MPa. Simply switching to Portland Limestone Cement (PLC) in Mix 2 provided a modest increase to 30.2 MPa, likely due to the finer particles of PLC creating a denser paste microstructure. The most significant finding is the performance of the mixes with reduced C/A ratios. The strength progressively increased as the ratio decreased, peaking with Mix 4 (C/A = 0.165), which achieved a 28-day compressive strength of 42.2 MPa. This represents a remarkable 49% increase over the Type II baseline and a 40% increase over the PLC baseline. This counterintuitive result—where less cement yields more strength—is attributed to the enhanced particle packing of the aggregates. A denser aggregate skeleton provides a more robust structure, reducing the reliance on the weaker cement paste for strength and minimizing microstructural voids.

When the C/A ratio was lowered further to 0.15, the strength began to decrease, suggesting that a C/A ratio of 0.165 represents the optimal balance between paste volume and aggregate packing for maximizing compressive strength in this system.

3-1-3- Flexural Strength

Flexural strength, or modulus of rupture, is a key indicator of a concrete's ability to resist cracking from bending stresses. The 28-day flexural strength results, presented in Table 5 and Figure 3, mirror the trend observed in compressive strength.

Table 5. Flexural strength test results for regular concrete

NO.	Name	Flexural strength (psi)
1	0.21 (Type II)	2.78
2	0.21 (PLC)	2.95
3	0.18 (PLC)	4.07
4	0.165 (PLC)	4.14
5	0.15a (PLC)	3.93
6	0.15b (PLC)	3.81

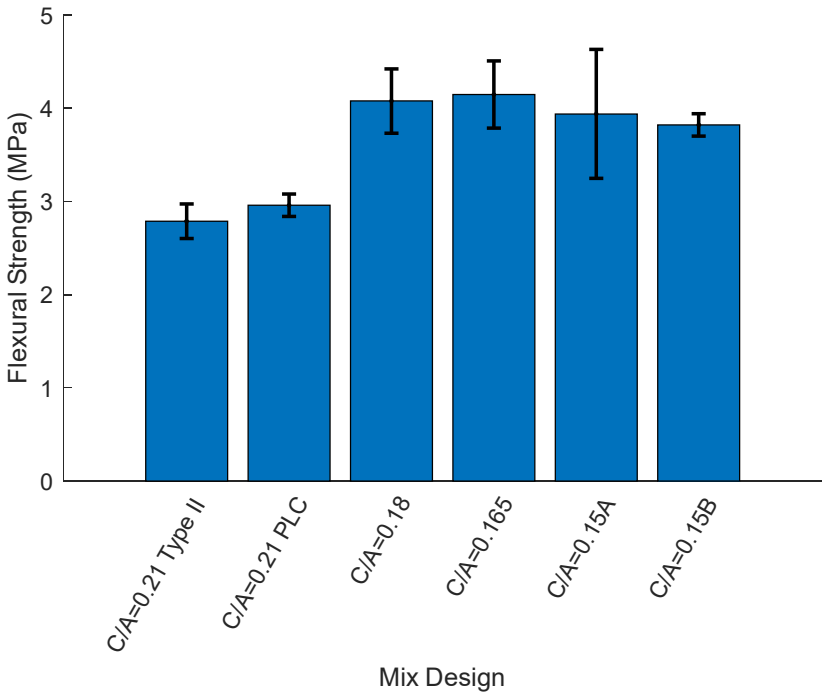

Figure 3. 28-day flexural strength results for regular concrete mixes.

The optimized mix with a C/A ratio of 0.165 (Mix 4) achieved the highest flexural strength of 4.14 MPa, a 49% improvement over the Type II baseline. This significant enhancement in bending resistance is crucial for applications like bridge decks, where flexural cracks are a primary durability concern. The improved aggregate interlock in the low-paste mixes creates a material that is more resistant to crack initiation and propagation. As with compressive strength, reducing the C/A ratio below 0.165 led to a decline in flexural performance, again highlighting 0.165 as the optimal ratio.

3-1-4- Durability Potential: Bulk Resistivity

Bulk resistivity is an excellent indicator of concrete's potential durability, as it measures the resistance to the flow of ions through its pore structure. Higher resistivity correlates to lower permeability, meaning it is more difficult for aggressive agents like chlorides to penetrate the concrete and initiate corrosion. The results at 28 and 56 days are shown in Table 6 and Figure 4.

Table 6. Bulk resistivity results for regular concrete

Paste to Agg.	Bulk Resistivity (Koh-Cm)-56 days	Bulk Resistivity (Koh-Cm)-28 days
0.21 (Type II)	21.2	14.5
0.21 (PLC)	23.1	15.4
0.18 (PLC)	23.7	15.8
0.165 (PLC)	24.2	16
0.15a (PLC)	24.4	16.2
0.15b (PLC)	24.5	16.4

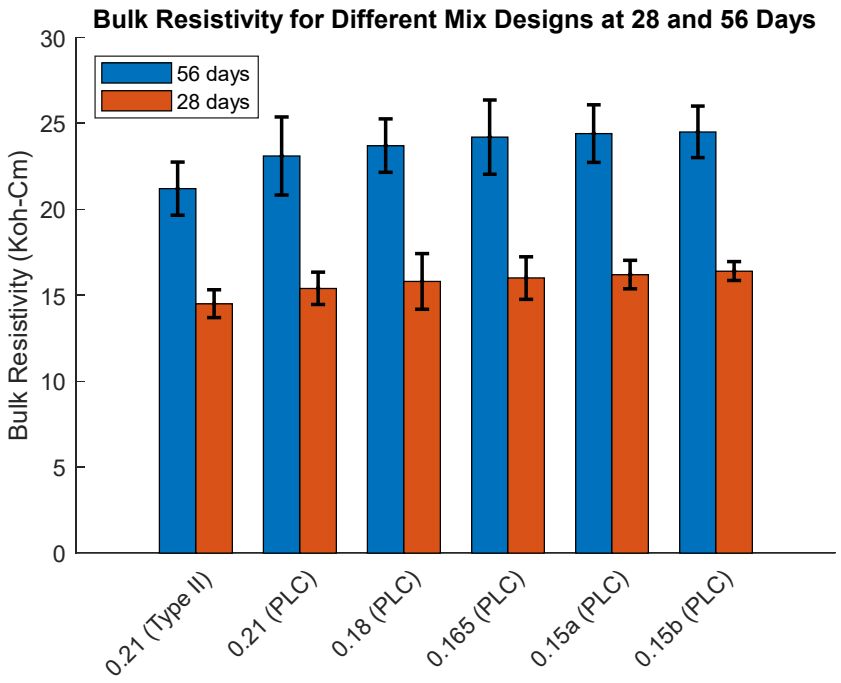

Figure 4. Bulk resistivity results for regular concrete at 28 and 56 days.

The data shows a clear and consistent trend: as the C/A ratio decreases, the bulk resistivity increases. At 56 days, the resistivity improved from 21.2 kΩ·cm for the baseline to 24.5

kΩ·cm for the mix with a C/A ratio of 0.15. This indicates that the denser microstructure achieved through aggregate optimization not only enhances strength but also creates a less permeable, more durable concrete matrix that is better equipped to resist chemical attack and extend the service life of the structure.

3-1-5- Dimensional Stability: Drying Shrinkage

The primary motivation of this research phase was to reduce shrinkage. Figure 5 presents the 22-day drying shrinkage results for the regular concrete mixes.

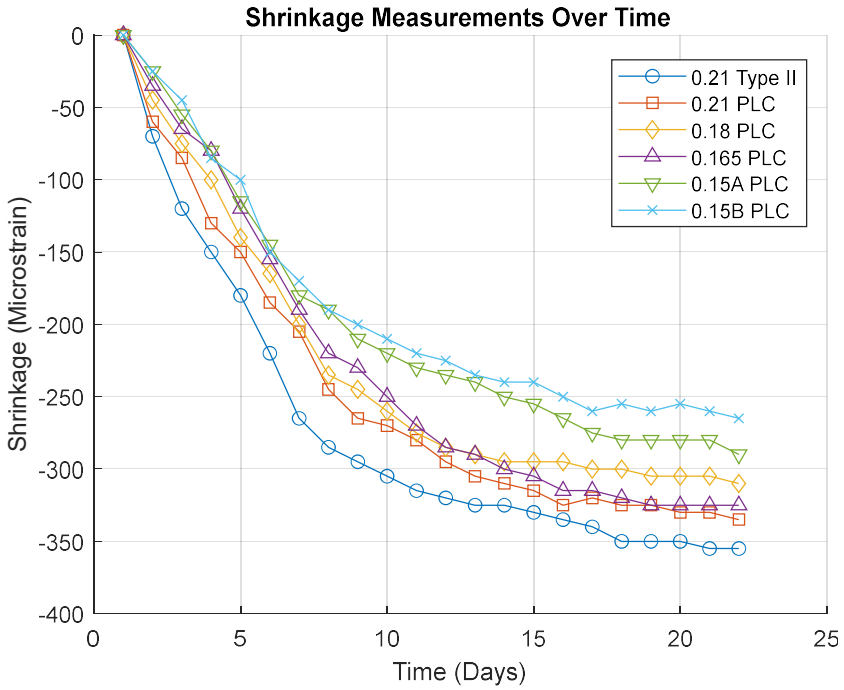

Figure 5. Shrinkage test results for regular concrete mixes over 22 days.

The results unequivocally demonstrate that reducing the volume of cement paste is a highly effective strategy for minimizing drying shrinkage. The baseline Type II mix exhibited the highest shrinkage, peaking at 355 microstrains. The optimized mixes showed progressively lower shrinkage as the C/A ratio was reduced. The mix with the lowest paste content (0.15b) had the lowest shrinkage, at 265 microstrains—a reduction of over 25% compared to the baseline. Since shrinkage is primarily a phenomenon of the cement paste, reducing the amount of paste directly reduces the overall volumetric change of the concrete. This is a

critical finding, as it provides a direct pathway to designing concrete with superior dimensional stability and a lower intrinsic tendency to crack.

3-2- Performance of Internally Cured Concrete with Lightweight Aggregate (LWA)

This section evaluates the effect of incorporating pre-wetted LWA as an internal curing agent. The goal was to determine if LWA could further reduce shrinkage without significantly compromising the mechanical properties established in the optimized regular concrete mixes.

3-2-1- Compressive Strength

Figures 6, 7, and 8 show the compressive strength development for mixes with 5%, 10%, and 15% LWA replacement, respectively.

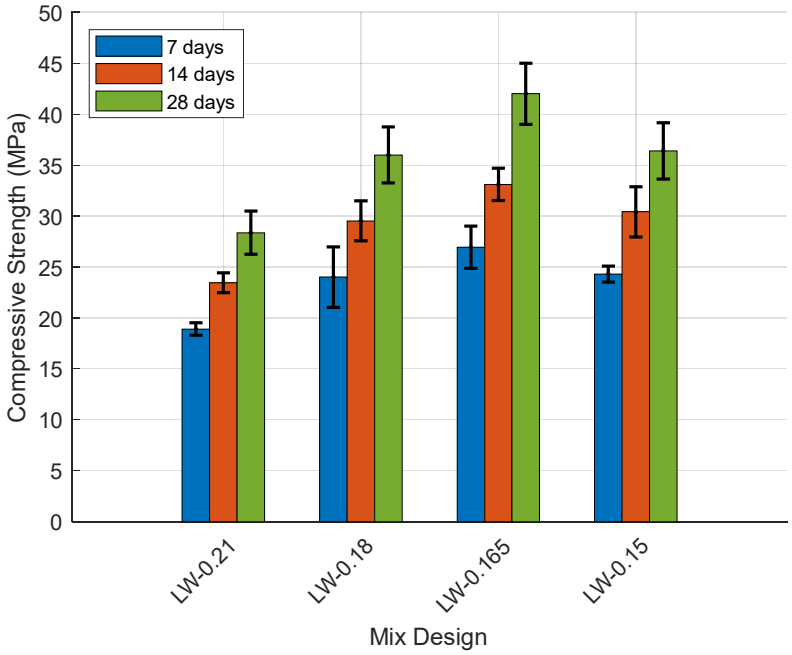

Figure 6. Compressive strength development for mixes with 5% LWA.

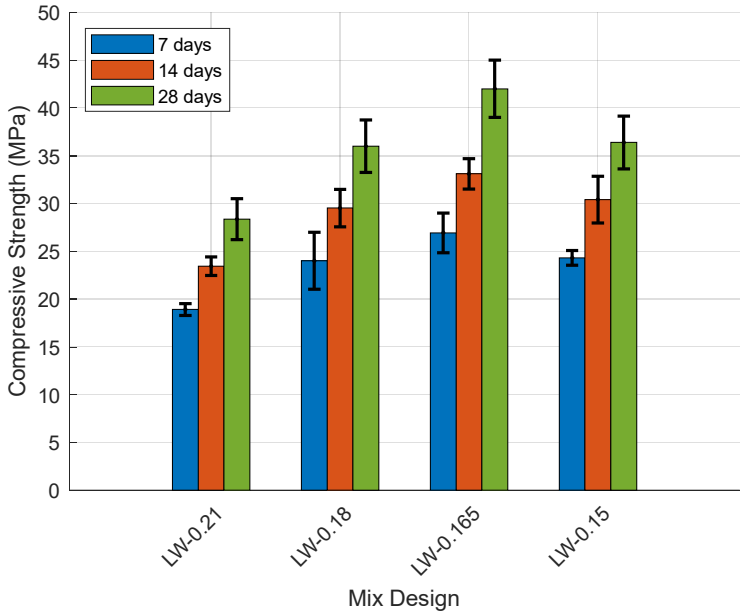

Figure 7. Compressive strength development for mixes with 10% LWA.

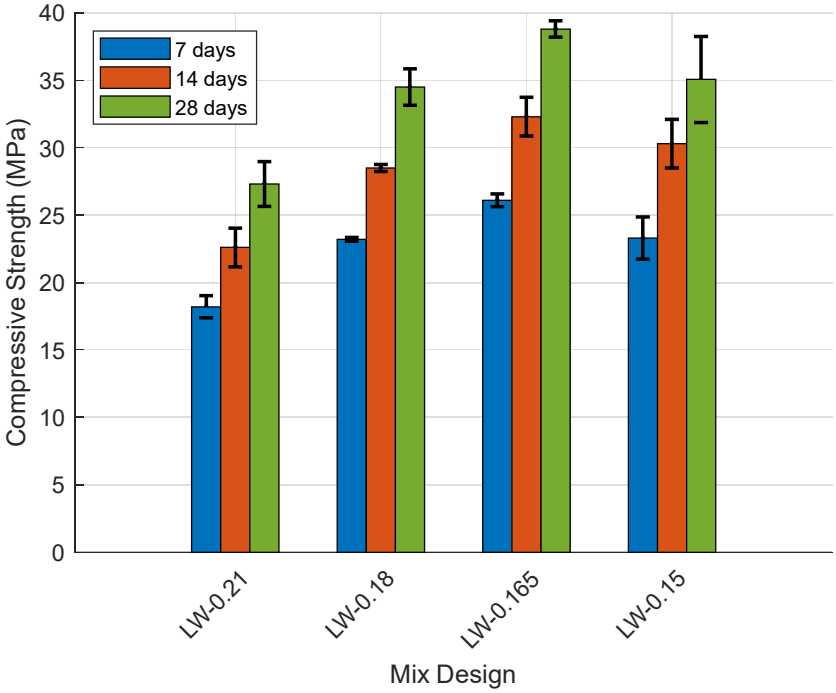

Figure 8. Compressive strength development for mixes with 15% LWA.

The introduction of LWA, which is inherently weaker than standard aggregate, generally resulted in a slight reduction in compressive strength compared to the optimized regular

concrete. However, the strengths achieved were still exceptionally high and far exceeded typical requirements. For instance, in the 15% LWA group, the mix with a C/A ratio of 0.165 achieved a 28-day strength of 34.5 MPa. While this is lower than the 42.2 MPa achieved without LWA, it is still a very robust value. The results indicate that the benefit of internal curing can be achieved with a manageable and predictable trade-off in compressive strength.

3-2-2- Flexural Strength

The 28-day flexural strength results for the LWA mixes are compiled in Figure 9.

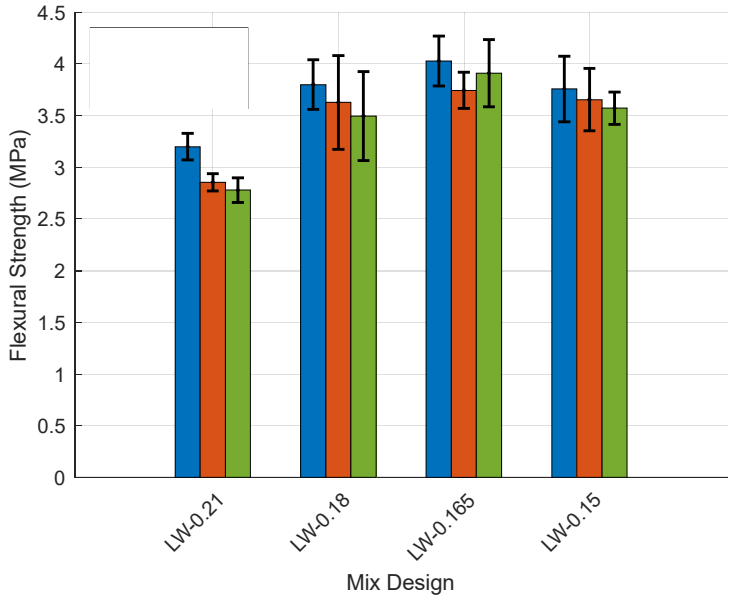

Figure 9. 28-day flexural strength for lightweight concrete mixes with 5%, 10%, and 15% LWA.

Similar to compressive strength, adding LWA tended to slightly decrease flexural strength. The 0.165 PLC mix, which was the top performer in regular concrete, showed a consistent trend: 3.80 MPa at 5% LWA, 3.63 MPa at 10% LWA, and 3.91 MPa at 15% LWA. Interestingly, the flexural strength for the 0.165 PLC mix remained high across all LWA percentages, peaking at 15% LWA. This suggests that for bending resistance, the benefits of internal curing from a higher volume of LWA may help offset the reduction in strength from the aggregate itself, possibly by reducing microcracking at the paste-aggregate interface.

3-2-3- Durability Potential: Bulk Resistivity

The bulk resistivity results for the LWA mixes, shown in Figure 10, demonstrate excellent durability potential.

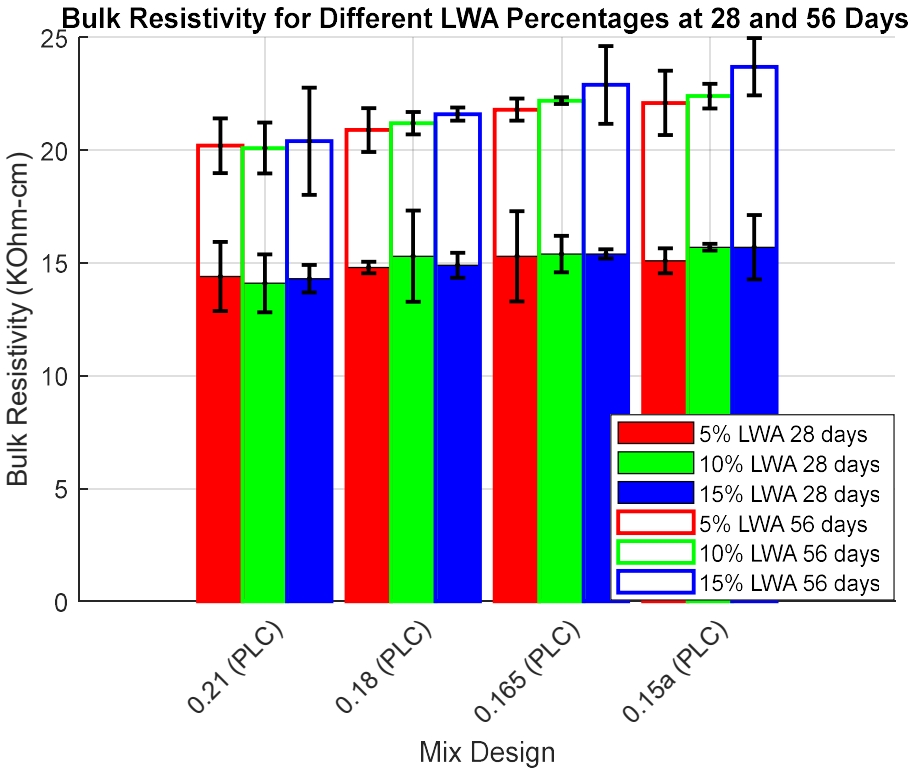

Figure 10. Bulk resistivity for lightweight concrete mixes at 28 and 56 days.

The resistivity values for the LWA mixes were slightly lower than their regular concrete counterparts but remained high overall. For example, the 0.15 PLC mix with 15% LWA recorded a 56-day resistivity of 23.7 kΩ·cm. This is only a minor reduction from the 24.5 kΩ·cm of the regular mix and indicates a highly impermeable microstructure. The internal curing provided by the LWA likely contributes to a more complete hydration of the cement particles, helping to refine the pore structure and maintain high resistance to ion penetration.

3-2-4- Shrinkage Mitigation

The primary purpose of adding LWA was to reduce shrinkage. The results, presented in Figures 11, 12, and 13, confirm its effectiveness.

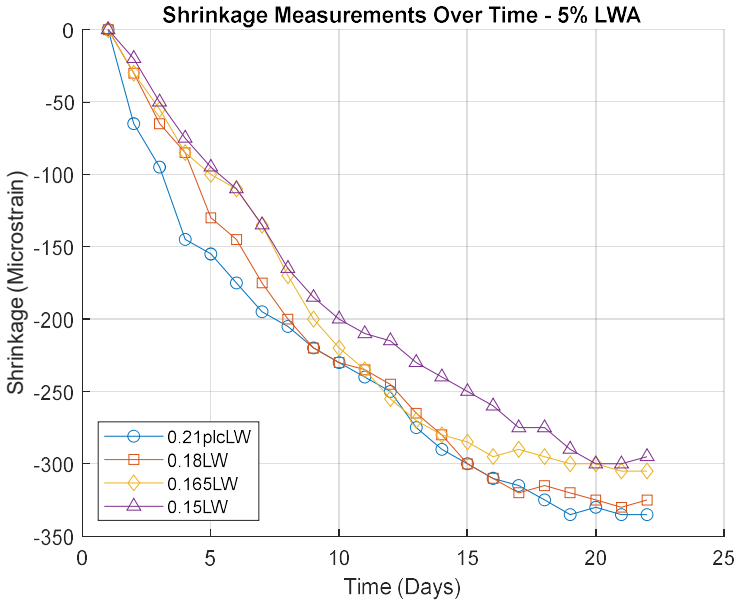

Figure 11. Shrinkage test results for mixes with 5% LWA.

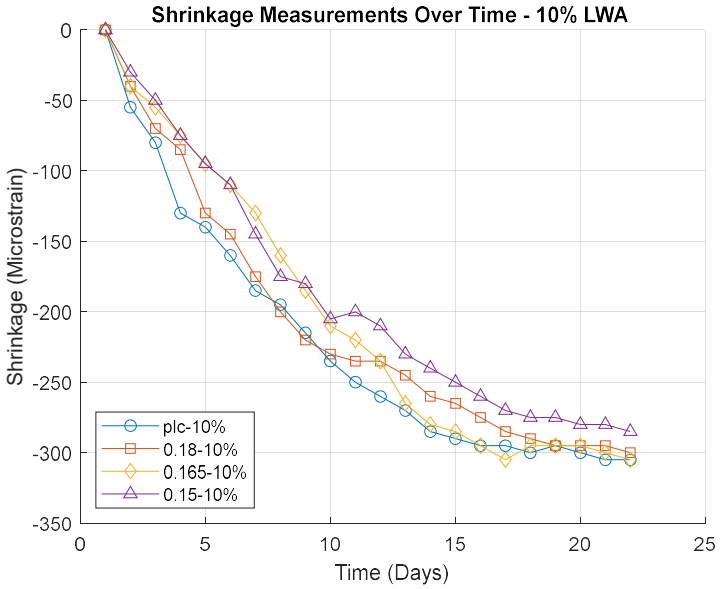

Figure 12. Shrinkage test results for mixes with 10% LWA.

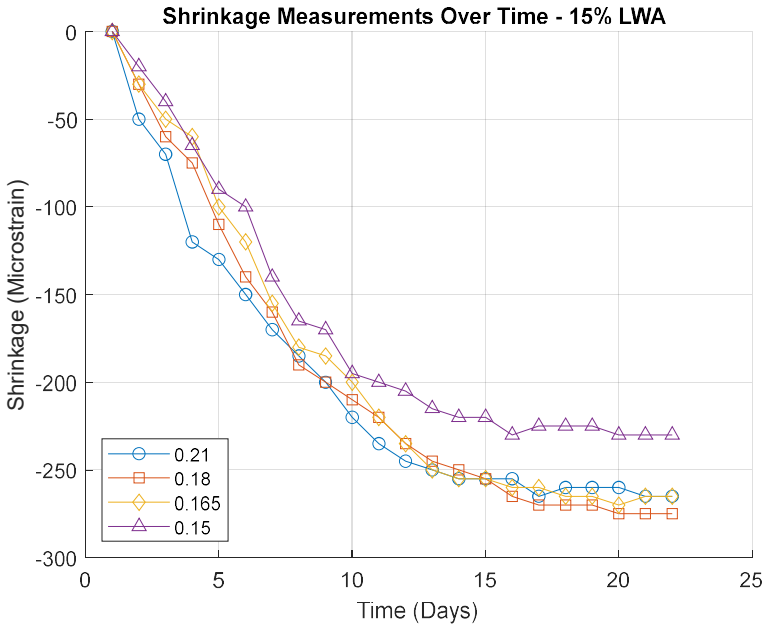

Figure 13. Shrinkage test results for mixes with 15% LWA.

Across all C/A ratios, the addition of LWA led to a further reduction in shrinkage compared to the already optimized regular concrete mixes. The effect was most pronounced at the highest replacement level. The mix with a C/A ratio of 0.15 and 15% LWA exhibited the lowest shrinkage of all mixes tested. This is because the LWA acts as a network of internal water reservoirs, releasing moisture as the surrounding paste begins to dry and self-desiccate. This process maintains a higher internal relative humidity, counteracting the driving forces of both autogenous and drying shrinkage.

3-3- Comparative Analysis: The Synergy of Mix Optimization and Internal Curing

To synthesize the findings, it is crucial to directly compare the performance of the optimized regular concrete with the internally cured lightweight concrete. Table 7 and Figure 14 provide this comparison for the mixes with a C/A ratio of 0.15.

Table 7. Comparison between regular and LWA concrete (C/A Ratio = 0.15)

Type of Concrete	Compressive strength (28 days)	Flexural strength	Last day shrinkage	56 days bulk resistivity
Regular	5424	571	290	24.5
5% LW	5279	545	285	22.1
10% LW	5136	530	265	22.4
15% LW	5084	518	230	23.7

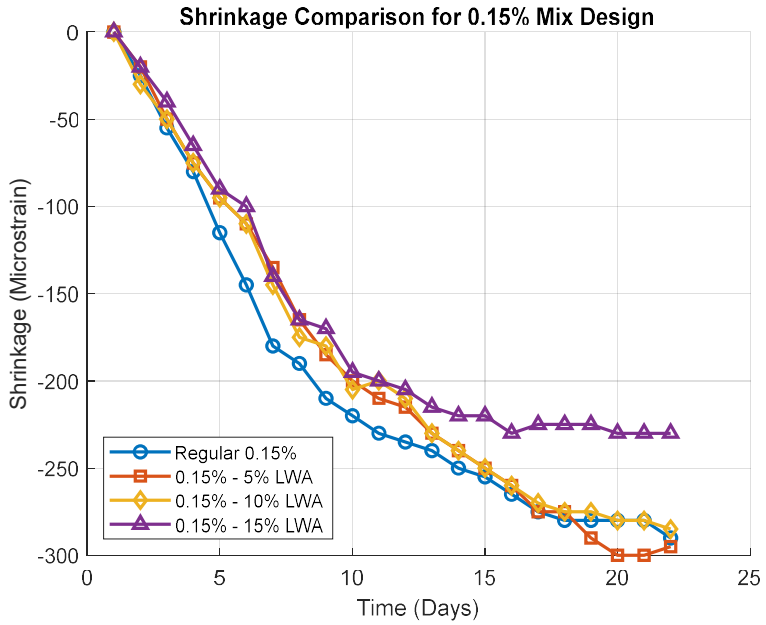

Figure 14. Shrinkage comparison between regular concrete and lightweight concrete mixes (C/A Ratio = 0.15).

This comparison highlights the key trade-offs and synergies. Adding 15% LWA resulted in a modest 6.3% decrease in compressive strength and a 9.3% decrease in flexural strength compared to the optimized regular concrete. However, this was accompanied by a significant **20.7% further reduction in shrinkage**. The durability, as measured by bulk resistivity, remained excellent, with only a 3.3% reduction.

This analysis reveals that a combined approach is most effective. First, optimizing the aggregate gradation and reducing the paste content creates a concrete that is inherently

stronger, more durable, and less prone to shrinkage. Second, introducing LWA onto this optimized platform provides an additional, powerful mechanism to mitigate the remaining shrinkage with only a minor and acceptable compromise in mechanical properties. The C/A = 0.165 mix with 15% LWA emerges as a particularly well-balanced design, offering an optimal combination of high strength, excellent durability, and superior dimensional stability.

3-4- Sustainability Investigation

A key driver for this research was to reduce the environmental impact of concrete, primarily by lowering its cement content. A Life Cycle Assessment (LCA) was conducted using TRACI 2.1 methodologies to compare the environmental performance of four key mix designs.

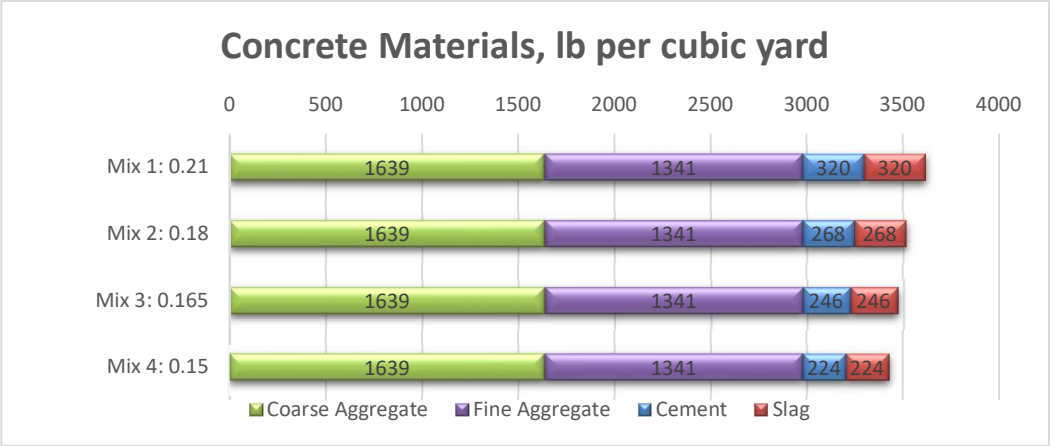

Figure 15. Mix designs selected for sustainability investigation.

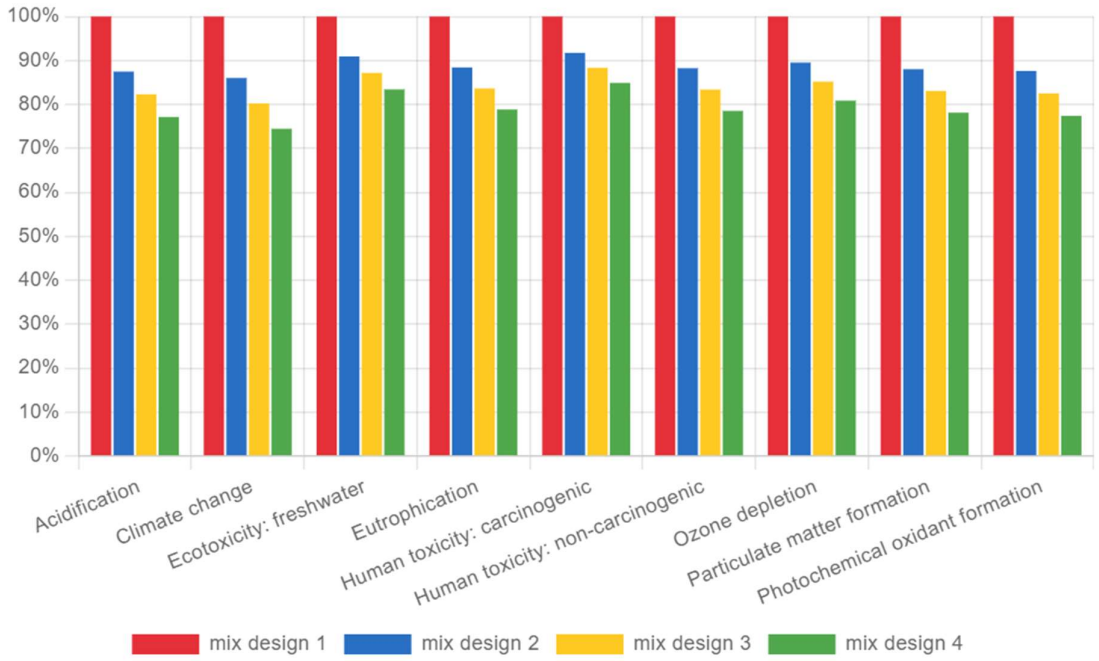

Figure 16. Normalized environmental impact analysis for the four selected mix designs across multiple categories.

The results of the LCA, shown in Figure 16, are clear. Across all environmental impact categories—including global warming potential (climate change), acidification, eutrophication, and toxicity—the mixes with lower cement content performed significantly better. Mix Design 4 (C/A = 0.15) consistently exhibited the lowest environmental impact. Focusing on Global Warming Potential (GWP), which is dominated by CO_2 emissions from cement production, the benefits are substantial. As shown in Figure 17, reducing the C/A ratio from 0.21 (Mix 1) to 0.15 (Mix 4) resulted in a **30% reduction in CO_2 emissions** from clinker production (from 213 kg CO_2-Eq to 149 kg CO_2-Eq per cubic meter of concrete).

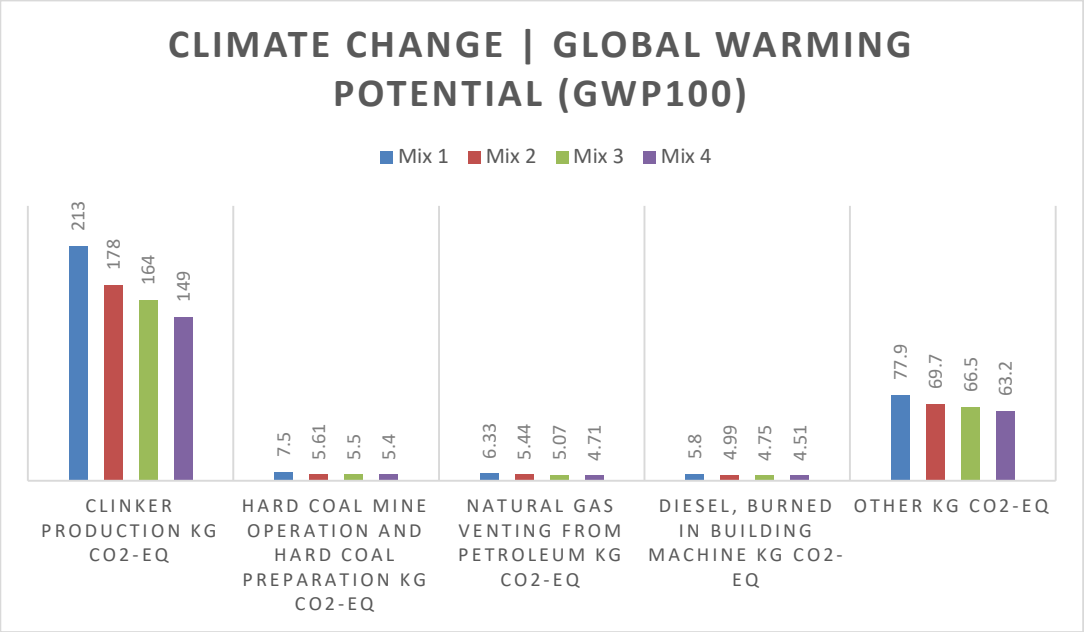

Figure 17. Breakdown of Global Warming Potential (GWP100) by source for the four mix designs.

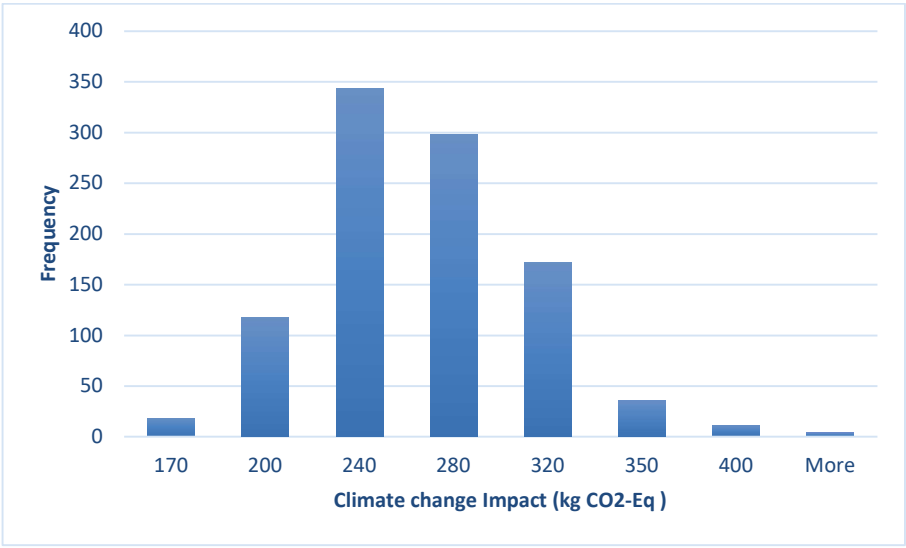

Figure 18. Sensitivity analysis showing the direct correlation between cement amount and climate change impact (GWP).

The sensitivity analysis in Figure 18 further reinforces this conclusion, illustrating a direct and powerful correlation between the amount of cement used and the concrete's GWP. This sustainability analysis confirms that the strategies employed in this research to enhance mechanical performance and durability—namely, the reduction of cement content through

aggregate optimization—are the same strategies that lead to a more environmentally responsible and sustainable concrete.

Chapter 4:Results and Discussion: Thermal Strain Analysis in Composite Bridge Decks

While optimizing the concrete mix design is fundamental to reducing intrinsic shrinkage, the overall performance of a concrete bridge deck is also heavily influenced by its interaction with the supporting structure. This chapter presents the results from the second phase of the research, which focused on quantifying and mitigating the risk of cracking due to thermal stresses in a composite concrete-on-steel-girder bridge. By analyzing in-situ temperature data and developing a computational model, this investigation assesses the magnitude of thermally induced strains and evaluates the effectiveness of potential mitigation strategies.

4-1- In-Situ Temperature Profiles

The first step in the analysis was to understand the thermal environment experienced by a real-world bridge structure. Temperature data was collected over approximately 13 days from both the newly placed concrete deck and the underlying steel beam. The recorded temperature profiles are presented in Figure 19.

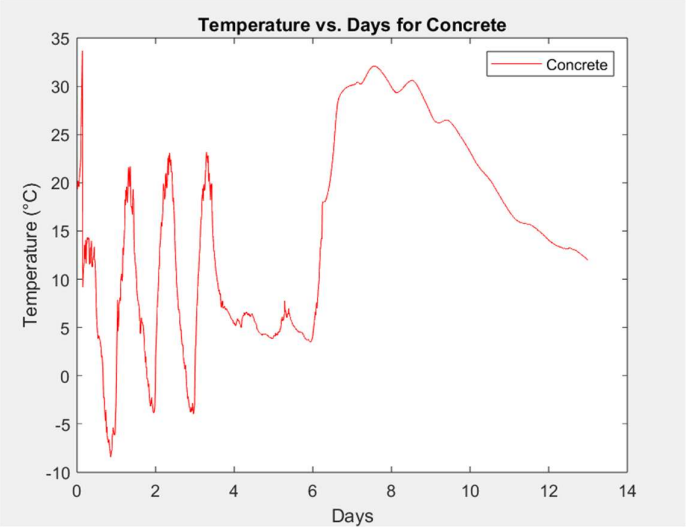

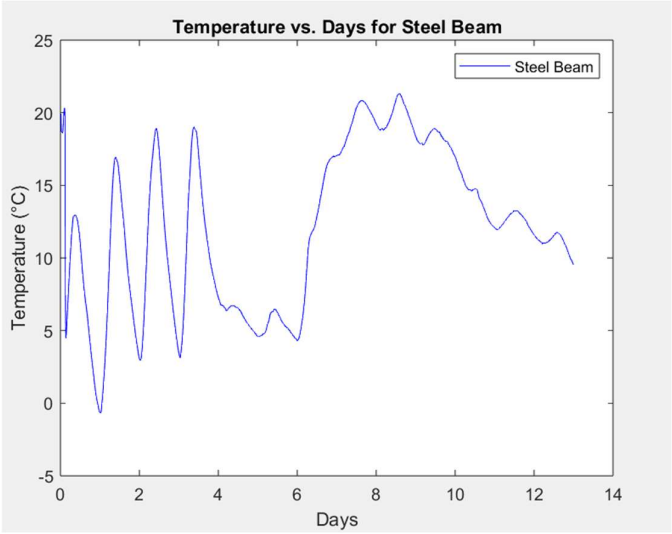

Figure 19. Measured temperature profiles over 13 days for the concrete deck (top) and the supporting steel beam (bottom).

The data reveals several key phenomena. During the first 24-48 hours, the concrete temperature rises significantly due to the exothermic heat of hydration, reaching temperatures well above the ambient conditions. The steel beam temperature, in contrast, more closely follows the diurnal (daily) temperature swings. After the initial heat of hydration period, both the concrete and steel temperatures fluctuate with the daily cycle, but the more massive concrete deck exhibits a dampened thermal response compared to the steel.

4-2- Thermal Gradient Analysis

The critical factor for inducing stress in a composite structure is not the absolute temperature, but the *difference* in temperature between the constituent materials. A significant temperature differential between the warmer concrete deck and the cooler steel beam forces the concrete to contract more than the steel, inducing tensile stress in the concrete. Figure 20 plots the temperature difference between the concrete and steel over the first 7 days.

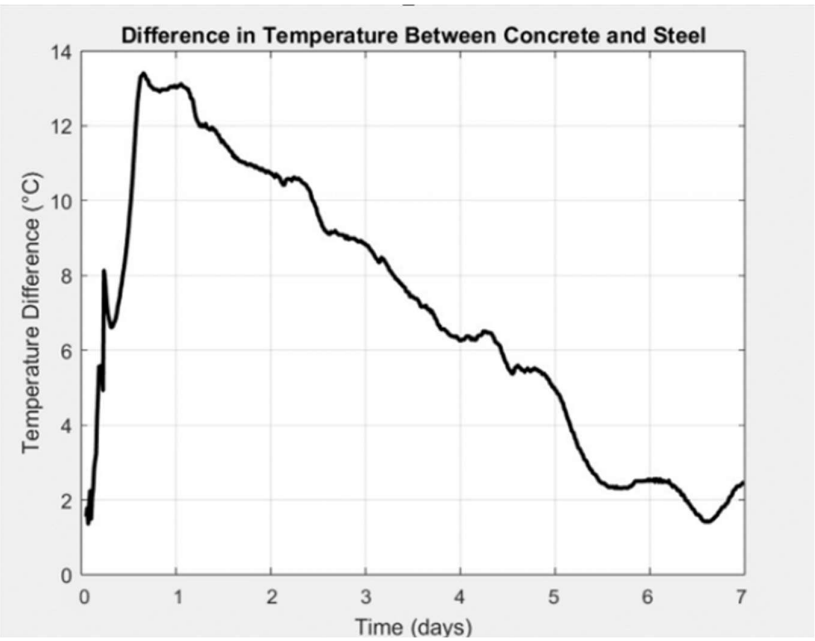

Figure 20. Calculated temperature difference (ΔT) between the concrete deck and steel beam during the first 7 days.

The analysis shows a substantial thermal gradient developing almost immediately after placement. The temperature difference peaks at nearly 14°C within the first 24 hours, driven by the heat of hydration in the concrete. This large and sustained temperature differential is the primary driver of early-age thermal stress and creates a high-risk period for crack formation.

4-3- Time-Dependent Material Property Development

To accurately assess the concrete's ability to resist thermal stress, it is essential to model the development of its mechanical properties over time. Using the models specified in the methodology (ACI 209, ACI 318, and Raphael 1984), the time-dependent evolution of the concrete's compressive strength and modulus of elasticity was calculated. The development curves are shown in Figure 21.

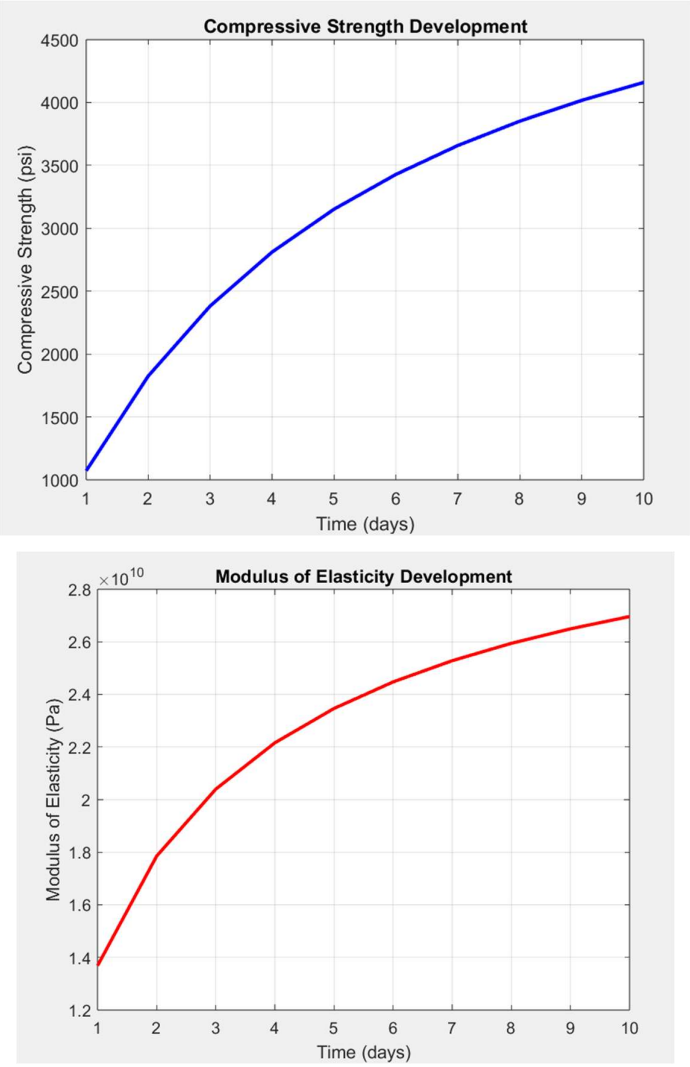

Figure 21. Modeled development of compressive strength (top) and modulus of elasticity (bottom) in the concrete over the first 10 days.

These models show the rapid gain in stiffness and strength during the first few days of curing. However, during the most critical period—the first 24-72 hours when thermal gradients are highest—the concrete has only developed a fraction of its final strength and stiffness, making it particularly vulnerable to cracking. The allowable tensile strain capacity of the concrete, which is derived from these properties, is therefore at its lowest when the thermally induced tensile strains are at their highest.

4-4- Cracking Risk Assessment: Total Strain vs. Capacity

The core of the analysis was to compare the total tensile strain imposed on the concrete deck against its evolving tensile strain capacity. The total strain is the sum of the inherent drying/autogenous shrinkage strain and the thermally induced strain.

Figure 22 shows the calculated thermal strain component alongside the concrete's allowable tensile strain capacity.

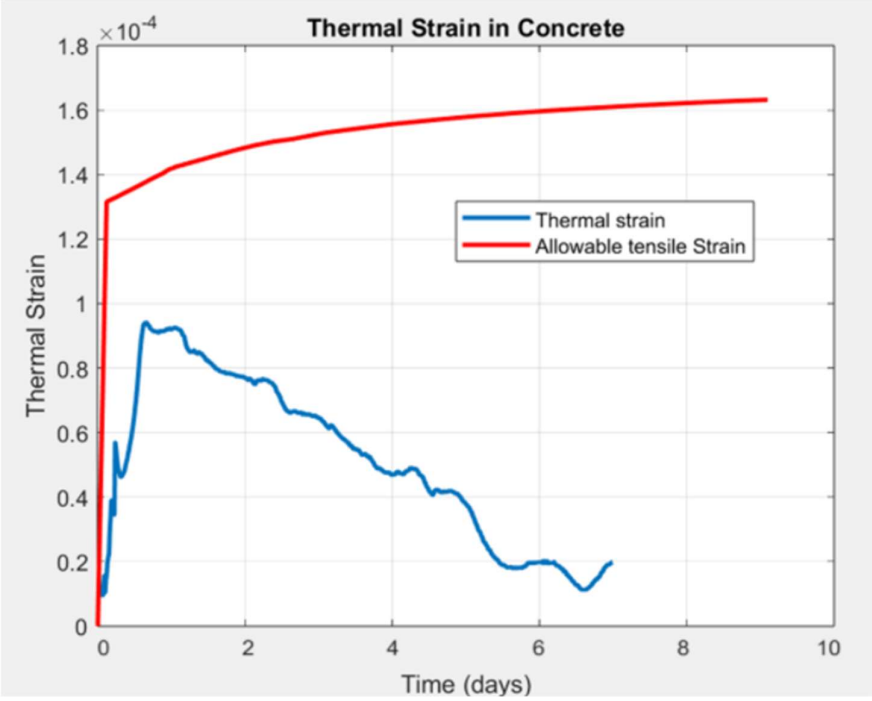

Figure 22. Comparison of the calculated thermal strain induced in the concrete versus the concrete's allowable tensile strain capacity over time.

This comparison reveals a critical situation: the thermal strain alone, driven by the temperature differential, approaches the concrete's cracking limit within the first day. When the inherent shrinkage strain of the concrete is added to this thermal strain, the total strain exceeds the material's capacity. Figure 23 shows the final analysis, plotting the thermal strain, shrinkage strain, and the resulting total strain against the allowable limit.

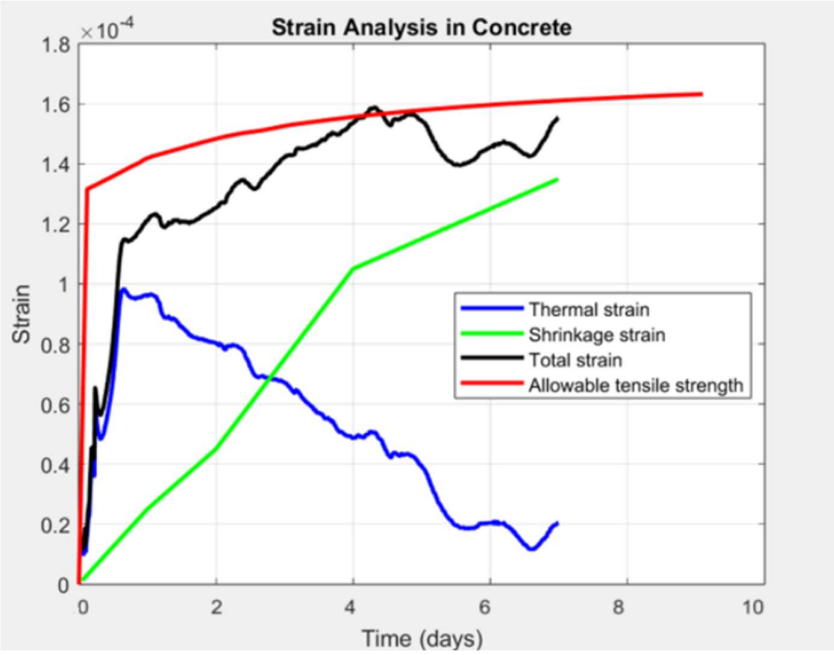

Figure 23. Total strain analysis, showing the contribution of thermal strain and shrinkage strain. The total strain (black line) exceeds the allowable tensile strength (red line), indicating a high probability of cracking.

The results from this analysis are unequivocal. The black line, representing the total strain on the concrete, clearly crosses the red line, representing the concrete's tensile capacity, at approximately day 3.5 and remains above it. This indicates that under the measured field conditions, the combined effects of thermal gradients and material shrinkage will induce tensile stresses that are sufficient to cause cracking in the concrete deck. This confirms that even a well-designed concrete mix can be compromised by uncontrolled thermal forces in a composite structure.

4-5- Evaluation of Thermal Mitigation Strategies

Given the high risk of cracking identified, the final step of the analysis was to model the effectiveness of a potential mitigation strategy: applying heat to the structure to reduce the temperature differential between the concrete and steel. Figure 24 shows the calculated thermal strain under scenarios where the temperature difference is artificially reduced by 1°C, 2°C, 3°C, 4°C, and 5°C.

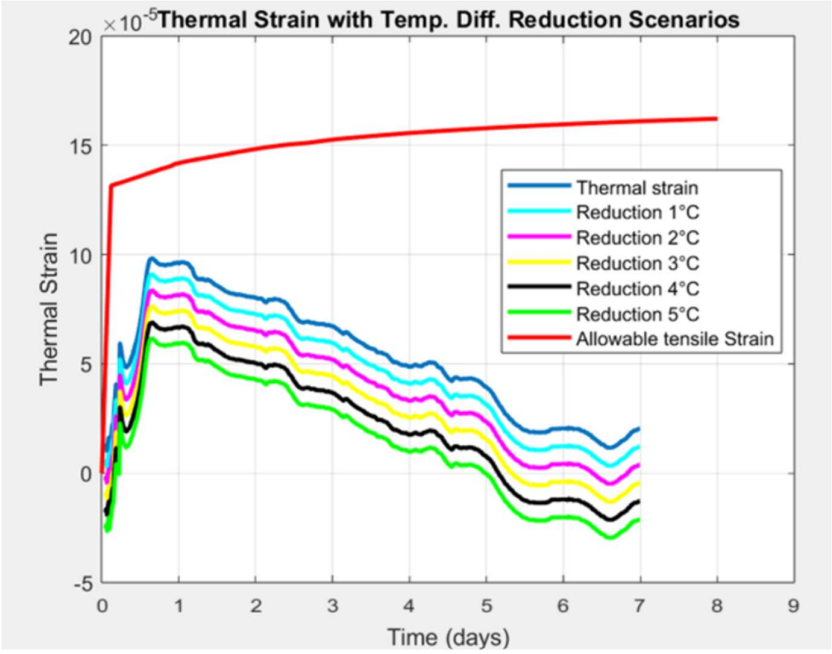

Figure 24. Modeled effect of reducing the temperature differential on the resulting thermal strain in the concrete.

The results of this simulation are highly encouraging. Each degree of reduction in the temperature differential provides a corresponding, significant reduction in the peak thermal strain. By reducing the temperature difference by 4°C to 5°C, the peak thermal strain can be lowered substantially. This reduction would, in turn, keep the *total* strain (thermal + shrinkage) below the concrete's allowable tensile capacity, effectively preventing the formation of early-age thermal cracks. This analysis provides a quantitative basis for specifying thermal control measures, such as heated enclosures or girder heating, during cold-weather concreting operations to ensure the long-term durability of the bridge deck.

Chapter 5: Results and Discussion: Performance Enhancement with Cellulose Nanofibrils (CNF)

This chapter presents the results from the third phase of the research, which investigated the use of Cellulose Nanofibrils (CNF) as a sustainable, high-performance admixture for concrete. The primary objectives were to evaluate the effect of various CNF dosages on the mechanical properties and shrinkage behavior of concrete and to identify an optimal dosage for practical applications. Concrete specimens were prepared with CNF dosages of 0%, 0.1%, 0.2%, 0.3%, 0.4%, and 0.5% by weight of cement.

5-1- Effect on Mechanical Properties

The influence of CNF on the concrete's ability to withstand structural loads was evaluated through compressive and flexural strength testing.

5-1-1- Compressive Strength

Compressive strength was tested at 7, 14, and 28 days according to ASTM C39. The results showed that strength increased with the addition of CNF, peaking at a dosage of 0.3%. At this optimal level, the 28-day compressive strength demonstrated a **16% increase** compared to the control mix. However, concentrations above 0.3% led to a decline in strength, which is likely caused by challenges in achieving uniform fiber dispersion, leading to agglomeration.

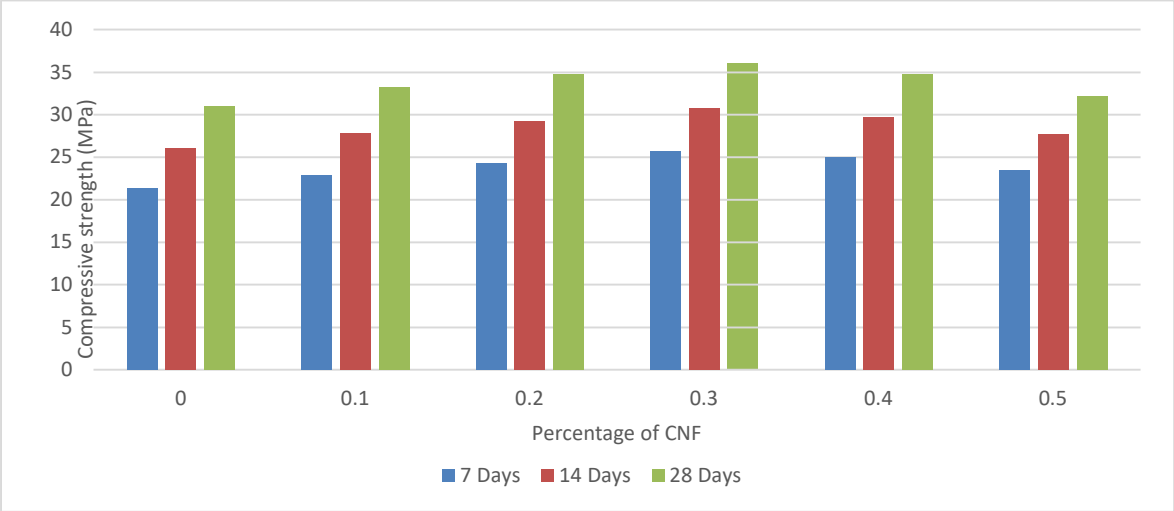

Figure 25. 28-day compressive strength of concrete as a function of CNF dosage.

5-1-2- Flexural Strength

Flexural strength, a critical indicator of a material's resistance to cracking from bending, was tested at 28 days (ASTM C78). The results showed a similar and even more pronounced trend. The peak performance was observed at the 0.3% CNF dosage, which yielded a remarkable **28% increase in flexural strength** over the control specimen. This significant improvement highlights CNF's effectiveness in bridging microcracks, thereby enhancing the concrete's toughness and ability to resist fracture.

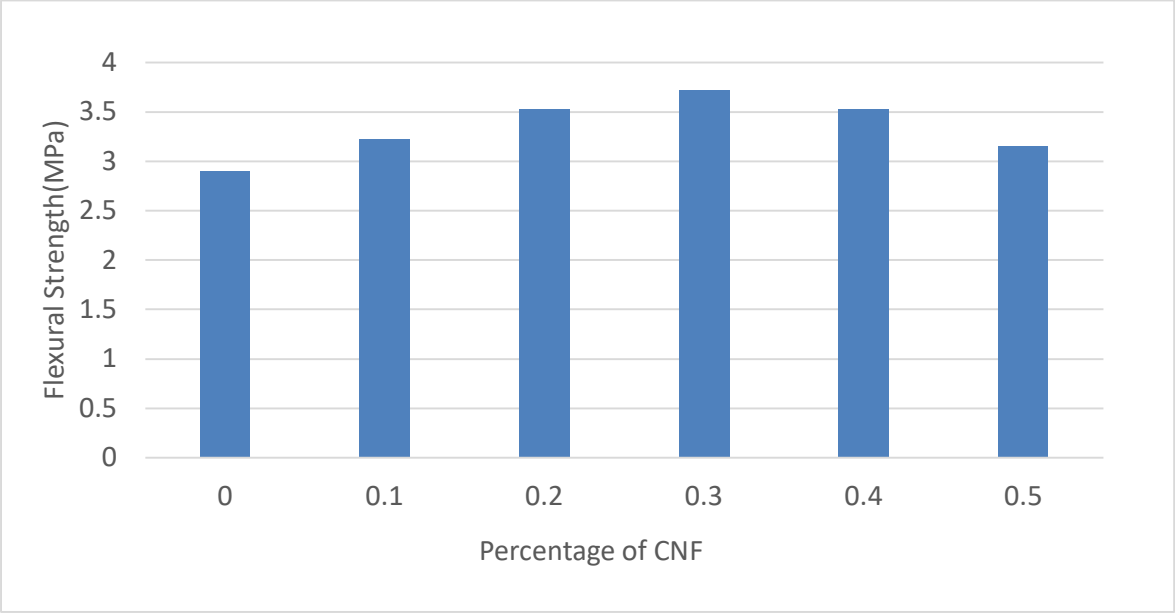

Figure 26. 28-day flexural strength of concrete as a function of CNF dosage.

5-2- Effect on Shrinkage Behavior

A primary motivation for this study was to address early-age shrinkage, a leading cause of concrete cracking. Drying shrinkage was monitored for 28 days per ASTM C157. All mixes containing CNF showed a reduction in shrinkage compared to the control. The most effective performance was achieved with the 0.3% CNF mix, which resulted in a **17% reduction in 28-day drying shrinkage**. This is attributed to the CNF's ability to retain water and act as an internal curing agent, combined with the physical restraint provided by the nanofiber network within the cement paste.

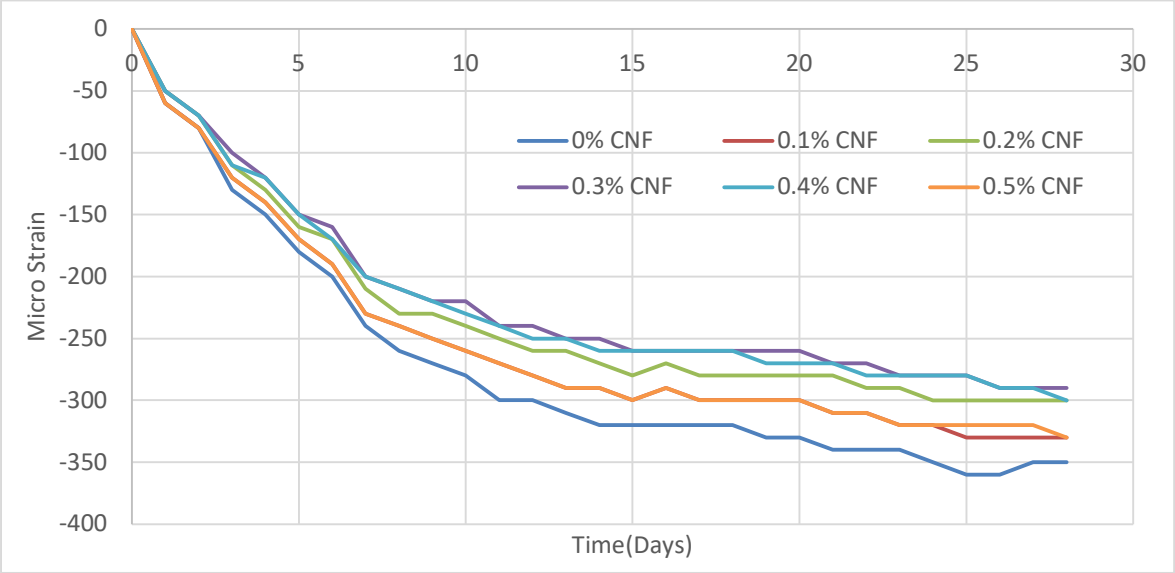

Figure 27. 28-day drying shrinkage as a function of CNF dosage.

5-3- Effect on Durability: Bulk Resistivity

To assess the impact of CNF on long-term durability, bulk resistivity measurements were taken at 28 and 56 days. Higher resistivity indicates a denser, less permeable microstructure, which enhances resistance to chloride ingress and corrosion. The results are presented in Table 8.

Table 8. Bulk Resistivity of CNF-Modified Concrete

CNF (%)	28-Day Bulk Resistivity (kΩ·cm)	56-Day Bulk Resistivity (kΩ·cm)
0	15.4	23.1
0.1	16.8	24.7
0.2	18.1	26.3
0.3	19	27.8
0.4	17.3	25.6
0.5	16.1	24.1

The data shows a clear improvement in durability with the addition of CNF, peaking at the 0.3% dosage. At 56 days, the 0.3% CNF mix achieved a bulk resistivity of 27.8 kΩ·cm, a 20% increase over the control mix's 23.1 kΩ·cm. This finding aligns with presentation data suggesting an improvement of 23%. The enhanced resistivity suggests that CNF contributes

to a more refined and tortuous pore structure, making it more difficult for aggressive ions to penetrate the concrete.

5-4- Microstructural Analysis and Discussion

The performance enhancements observed in the mechanical and durability tests can be explained by the influence of CNF at the microstructural level. The visual representation in Figure 30 illustrates the conceptual difference between poor dispersion at high dosages and good dispersion at the optimal dosage. The Scanning Electron Microscope (SEM) image in Figure 28 provides physical evidence of how CNF integrates with the cement hydration products.

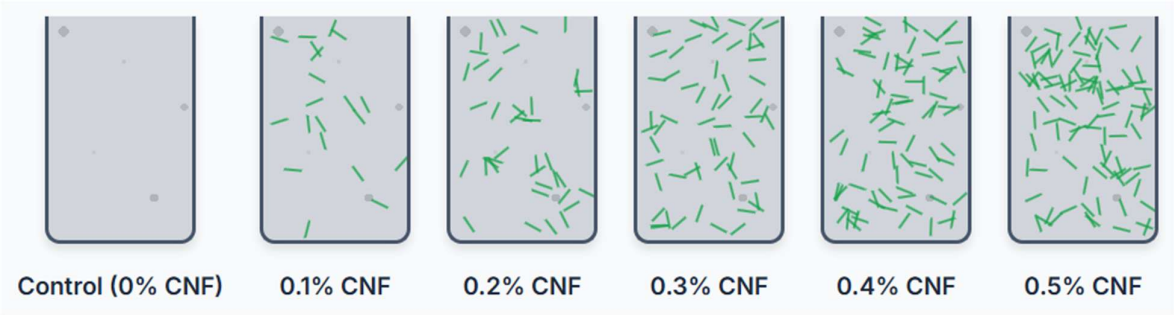

Figure 28. Conceptual illustration of CNF dispersion at varying dosages. The 0.3% level shows good distribution, while higher levels may lead to clumping (agglomeration).

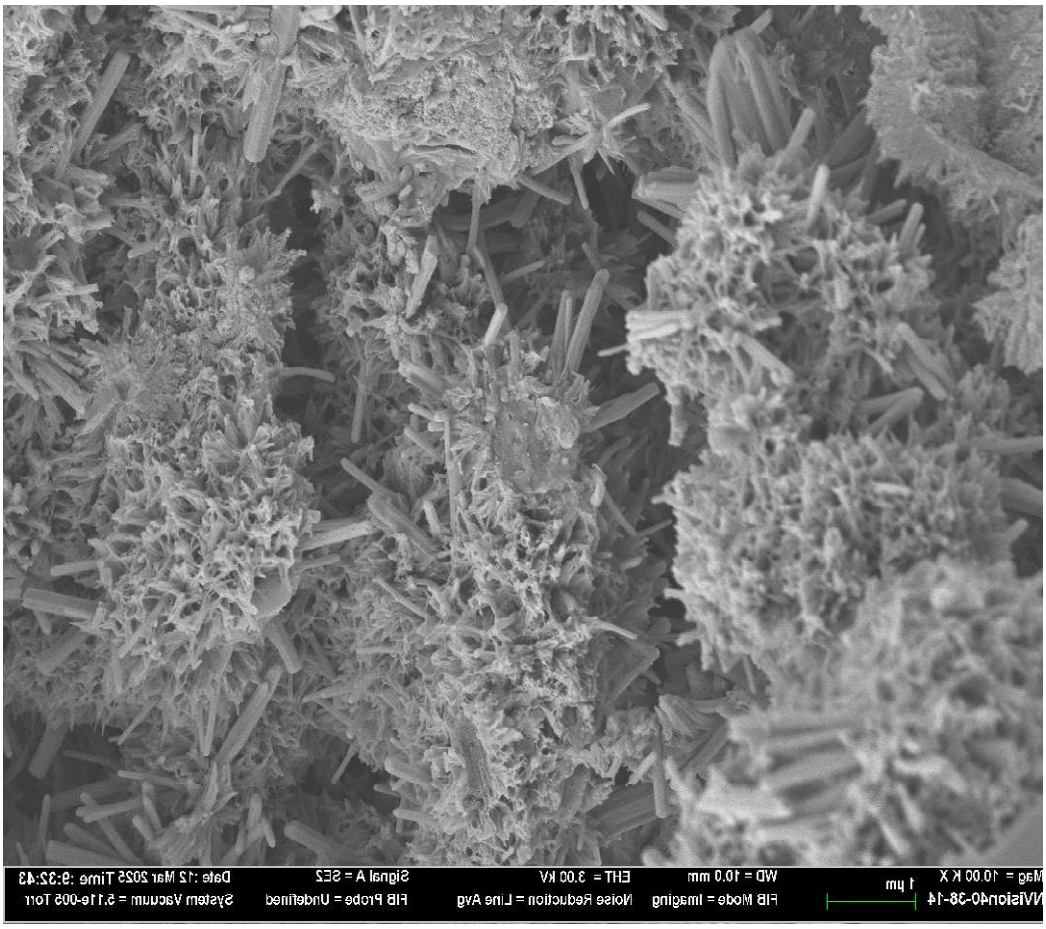

Figure 29. SEM image of the concrete microstructure showing the interaction between CNF and cement hydration products, which contributes to a reinforced matrix.

The combined results strongly indicate that CNF acts in several ways: by refining the pore structure, by providing nucleation sites for cement hydrates, and by bridging microcracks. At the optimal dosage of 0.3%, these mechanisms work in concert to produce a concrete that is stronger, more resistant to cracking, and more durable. This makes CNF a promising, sustainable admixture for developing the next generation of high-performance, crack-resistant concrete for critical infrastructure applications.

Chapter 6:Conclusions and Recommendations

This multi-phase research project was undertaken to develop a comprehensive, integrated set of solutions to mitigate early-age cracking and enhance the long-term durability of concrete for transportation infrastructure. By investigating fundamental mix design, real-world structural behavior, and advanced material additives, this study has yielded several key conclusions that lead to actionable recommendations for producing more resilient and sustainable concrete.

6-1- Conclusions

Based on the results presented in the preceding chapters, the following conclusions are drawn:

1. **Optimizing Aggregate Gradation and Reducing Cement Content is a Highly Effective Strategy for Improving Concrete Performance.** By applying the Tarantula Curve methodology to optimize the aggregate skeleton, it was possible to significantly reduce the cement-to-aggregate ratio. This led to a concrete that was simultaneously stronger (up to 49% increase in flexural strength), more durable (15% increase in bulk resistivity), and more dimensionally stable (over 25% reduction in shrinkage) than conventional mixes. The optimal balance for mechanical properties was found at a C/A ratio of 0.165.
2. **Internal Curing with Lightweight Fine Aggregates (LWA) Provides a Significant Additional Reduction in Shrinkage.** The introduction of pre-wetted LWA successfully provided an internal source of moisture, further reducing drying shrinkage by an additional 20.7% in optimized mixes. This substantial benefit was achieved with only a minor and acceptable trade-off in mechanical strength (e.g., a 6.3% reduction in compressive strength for 15% LWA replacement), making it a highly favorable strategy for shrinkage-critical applications.
3. **The Environmental Benefits of Optimized Mix Design are Substantial.** The Life Cycle Assessment (LCA) confirmed that the same strategies used to improve mechanical performance—namely, reducing the cement content—directly result in a more sustainable concrete. Reducing the C/A ratio from 0.21 to 0.15 lowered the

Global Warming Potential by approximately 30%, primarily by reducing the amount of CO_2-intensive clinker required.

4. **Uncontrolled Thermal Gradients in Composite Bridges Pose a Significant Cracking Risk.** The thermal analysis demonstrated that the temperature differential between a curing concrete deck and the supporting steel girders can induce tensile strains that exceed the concrete's early-age cracking capacity. This confirms that even a high-quality, low-shrinkage concrete mix can fail if placed in an adverse thermal environment without proper controls.
5. **Cellulose Nanofibrils (CNF) are a Viable Admixture for Enhancing Both Strength and Shrinkage Resistance.** The addition of CNF at a low dosage of 0.3% by weight of cement acted as an effective micro-reinforcement and internal curing aid. This resulted in a significant improvement in both flexural strength (+28%) and shrinkage resistance (-17%), providing another powerful tool for creating crack-resistant concrete.

6-2- Recommendations

Based on the conclusions of this comprehensive study, the following recommendations are proposed for consideration by transportation agencies and the construction industry:

1. **Adopt Optimized Aggregate Gradation for Concrete Specifications.** It is recommended that standard concrete specifications be updated to incorporate aggregate gradation optimization based on methodologies like the Tarantula Curve. This will facilitate the use of mixes with lower cement paste volumes, leading to inherently more durable and sustainable concrete without compromising performance. A target C/A ratio of approximately 0.165 should be considered for high-performance applications.
2. **Specify the Use of Internal Curing for Shrinkage-Sensitive Applications.** For structures where minimizing cracking is a top priority, such as bridge decks and large flatwork, the use of internal curing with pre-wetted lightweight fine aggregates should be specified. A replacement level of 10-15% of the fine aggregate is recommended to achieve a significant reduction in shrinkage.

3. **Implement Thermal Control Plans for Composite Bridge Deck Placements.** To mitigate the risk of early-age thermal cracking, it is strongly recommended that a thermal control plan be required for all composite bridge deck placements, especially during spring and fall construction when large ambient temperature swings are common. The plan should aim to limit the temperature differential between the concrete and steel girders to a maximum of 5°C, which can be achieved through methods such as heated enclosures or direct heating of the steel girders.
4. **Conduct Further Pilot Studies on the Use of CNF.** The promising results for CNF warrant further investigation. It is recommended that pilot-scale field trials be conducted to evaluate the performance and cost-effectiveness of CNF-enhanced concrete in real-world transportation applications. This could lead to the development of a new class of high-performance, crack-resistant concrete for critical infrastructure.

By implementing this multi-pronged set of recommendations—addressing material proportions, internal curing, thermal control, and advanced additives—it is possible to significantly extend the service life, improve the safety, and reduce the environmental impact of our nation's concrete infrastructure.

Acknowledgments

The authors gratefully acknowledge the support and funding provided by the Transportation Infrastructure Durability Center (TIDC), the Maine Department of Transportation (MDOT), and the Advanced Structures and Composites Center (ASCC), which were crucial in facilitating this research. Special thanks are also extended to the Civil Engineering Department of the University of Maine for their support throughout this study.

References:

1. Cao Q., Jia J., Zhang L., Hao Y., & Lv X. Experimental study of axial compression of reinforced concrete columns made by environment-friendly post-filling coarse aggregate process. Structural Concrete 2021;22(3):1671-1687. https://doi.org/10.1002/suco.202000271
2. Gholami S., Hu J., Kim Y., & Mamirov M. Performance of portland cement-based rapid-patching materials with different cement and accelerator types, and cement contents. Transportation Research Record Journal of the Transportation Research Board 2019;2673(11):172-184. https://doi.org/10.1177/0361198119852330
3. Guimarães A. Granular skeleton optimisation and the influence of the cement paste content in bio-based oyster shell mortar with 100% aggregate replacement. Sustainability 2024;16(6):2297. https://doi.org/10.3390/su16062297
4. Fang Q., Cheng J., Wen H., & Liu H. Numerical simulation analysis of the dynamic mechanical property of concrete based on 3d meso-mechanical model. Frattura Ed Integrità Strutturale 2018;12(45):1-13. https://doi.org/10.3221/igf-esis.45.01
5. Guan Z., Wang P., Li Y., Li Y., Hu B., & Wang Y. Mesoscale finite element modeling of mortar under sulfate attack. Materials 2022;15(15):5452. https://doi.org/10.3390/ma15155452
6. Ťažký M., Bodnárová L., Ťažká L., Hela R., Meruňka M., & Hlaváček P. The effect of the composition of a concrete mixture on its volume changes. Materials 2021;14(4):828. https://doi.org/10.3390/ma14040828
7. Burgmann S. Impact of crushed natural and recycled fine aggregates on fresh and hardened mortar properties. Construction Materials 2023;4(1):37-57. https://doi.org/10.3390/constrmater4010003
8. Alkhaly Y., Khairullah K., Zulfhazli Z., Mardiah A., & Ariska D. Utilizing crushed clinker brick waste as coarse aggregate to produce concrete with compressive strengths up to 40 mpa by adjusting the gradation curve. International Journal of Engineering Science and Information Technology 2023;3(1):78-85. https://doi.org/10.52088/ijesty.v3i1.437
9. Ghoddousi P., Javid A., & Sobhani J. A fuzzy system methodology for concrete mixture design considering maximum packing density and minimum cement content. Arabian Journal for Science and Engineering 2015;40(8):2239-2249. https://doi.org/10.1007/s13369-015-1731-9
10. Nayaju A. and Tamrakar N. Evaluation of fine aggregates from the budhi gandaki-narayani river, central nepal for mortar and concrete. Journal of Nepal Geological Society 2019;58:69-81. https://doi.org/10.3126/jngs.v58i0.24575

11. Ukala D. Effects of combined aggregate gradation on the compression strength and workability of concrete using fineness modulus. Journal of Applied Sciences and Environmental Management 2019;23(5):851. https://doi.org/10.4314/jasem.v23i5.13
12. Jiang W., Liu L., Cao W., Yang S., Liu S., & Li J. Prediction model of vca formed by the packing of hybrid lithological coarse aggregates used in sma. Materials 2022;15(24):8952. https://doi.org/10.3390/ma15248952
13. Li C., Wang F., Deng X., Li Y., & Zhao S. Testing and prediction of the strength development of recycled-aggregate concrete with large particle natural aggregate. Materials 2019;12(12):1891. https://doi.org/10.3390/ma12121891
14. Wang J., Zhang J., & Zhang J. Cement hydration rate of ordinarily and internally cured concretes. Journal of Advanced Concrete Technology 2018;16(7):306-316. https://doi.org/10.3151/jact.16.306
15. Guo L., Wang M., Zhong L., & Zhang Y. Calculation model for the mixing amount of internal curing materials in high-strength concrete based on modified multimoora. Science and Engineering of Composite Materials 2020;27(1):455-463. https://doi.org/10.1515/secm-2020-0048
16. Abdulrasool A., Mohammed S., Kadhim N., & Kadhim Y. Effect of attapulgite as internal curing in high-performance concrete with variable temperature curing to enhance mechanical properties. Iop Conference Series Earth and Environmental Science 2022;961(1):012054. https://doi.org/10.1088/1755-1315/961/1/012054
17. Abdulrasool A., Kadhim N., Mohammed S., & Alher A. The use of ceramics as an internal curing agent in high performance concrete with variable temperature curing to improve mechanical characteristics. Iop Conference Series Earth and Environmental Science 2022;961(1):012024. https://doi.org/10.1088/1755-1315/961/1/012024
18. Zhang J., Han Y., & Zhang J. Evaluation of shrinkage induced cracking in concrete with impact of internal curing and water to cement ratio. Journal of Advanced Concrete Technology 2016;14(7):324-334. https://doi.org/10.3151/jact.14.324
19. Chatale A. Study on replacement of fine aggregate with light weighted super absorbent material in internal curing concrete. International Journal for Research in Applied Science and Engineering Technology 2024;12(5):4574-4580. https://doi.org/10.22214/ijraset.2024.62625
20. Saad O., Ragab K., Elnawawy O., Alharbi Y., Abadel A., Talaat A.et al. Lightweight structural concrete. Journal of Engineering Research 2021. https://doi.org/10.36909/jer.12219
21. Internal curing and supplementary cementitious materials in bridge decks. 2019. https://doi.org/10.14359/51722453
22. Nair H., Ozyildirim H., & Sprinkel M. Development of a specification for low-cracking bridge deck concrete in virginia. Transportation Research Record Journal

of the Transportation Research Board 2017;2629(1):83-90. https://doi.org/10.3141/2629-11
23. Suwan T. and Wattanachai P. Properties and internal curing of concrete containing recycled autoclaved aerated lightweight concrete as aggregate. Advances in Materials Science and Engineering 2017;2017:1-11. https://doi.org/10.1155/2017/2394641
24. Chen H., Wu K., Tang C., & Huang C. Engineering properties of self-consolidating lightweight aggregate concrete and its application in prestressed concrete members. Sustainability 2018;10(1):142. https://doi.org/10.3390/su10010142
25. Zhang P., Xie N., Cheng X., Li F., Hou P., & Wu Y. Low dosage nano-silica modification on lightweight aggregate concrete. Nanomaterials and Nanotechnology 2018;8:184798041876128. https://doi.org/10.1177/1847980418761283
26. Karim F. Influence of internal curing with lightweight pumice fine aggregate on the mechanical properties of cement mortars. Construction 2022;2(2):104-113. https://doi.org/10.15282/construction.v2i2.8744
27. Castellanos N. and Rodríguez-Torres S. Evaluation of internal curing effects on concrete. Ingeniería E Investigación 2019;39(2). https://doi.org/10.15446/ing.investig.v39n2.76505
28. Samozbijajući beton s unutarnjom njegom i lakim agregatom. Journal of the Croatian Association of Civil Engineers 2016;68(4):279-285. https://doi.org/10.14256/jce.1137.2014
29. Salih A. and Abed Z. Assessing the effect of using porcelanite on compressive strength of roller compacted concrete. Journal of Engineering 2023;20(10):16-28. https://doi.org/10.31026/j.eng.2014.10.02
30. Helsel M., Rangelov M., Montanari L., Spragg R., & Carrion M. Contextualizing embodied carbon emissions of concrete using mixture design parameters and performance metrics. Structural Concrete 2022;24(2):1766-1779. https://doi.org/10.1002/suco.202200634
31. Maryoto A., Gan B., Hermanto N., & Setijadi R. Effect of calcium stearate in the mechanical and physical properties of concrete with pcc and fly ash as binders. Materials 2020;13(6):1394. https://doi.org/10.3390/ma13061394
32. Tanyildizi M. Capillarity of concrete incorporating waste ceramic powder. Muş Alparslan Üniversitesi Fen Bilimleri Dergisi 2022;10(1):925-930. https://doi.org/10.18586/msufbd.1078690
33. Nalli B. and Vysyaraju P. Utilization of ceramic waste powder and rice husk ash as a partial replacement of cement in concrete. Iop Conference Series Earth and Environmental Science 2022;982(1):012003. https://doi.org/10.1088/1755-1315/982/1/012003

34. Mansour M. Compressive strength, temperature performance and shrinkage of concrete containing metakaolin. International Journal of Integrated Engineering 2023;15(6). https://doi.org/10.30880/ijie.2023.15.06.014
35. Kartini W., Astawa M., & Santosa H. Optimization of compressive strength and porosity of normal concrete using fly ash and alkaline activators. Ukarst 2022;6(1):102. https://doi.org/10.30737/ukarst.v6i1.2481
36. Yalcinkaya B., Špirek T., Bousa M., Louda P., Růžek V., Rapiejko C.et al. Unlocking the potential of biomass fly ash: exploring its application in geopolymeric materials and a comparative case study of bfa-based geopolymeric concrete against conventional concrete. Ceramics 2023;6(3):1682-1704. https://doi.org/10.3390/ceramics6030104
37. Kamaruddin S., Wan I., Jhatial A., & Lakhiar M. Chemical and fresh state properties of foamed concrete incorporating palm oil fuel ash and eggshell ash as cement replacement. International Journal of Engineering & Technology 2018;7(4.30):350. https://doi.org/10.14419/ijet.v7i4.30.22307
38. Campos H., Bellon A., Silva E., & Villatore M. Eco-efficient concrete, optimized by alfred's particle packing model, with partial replacement of portland cement by stone powder. Revista Ibracon De Estruturas E Materiais 2022;15(2). https://doi.org/10.1590/s1983-41952022000200005
39. Tang J. The effect of demolition concrete waste on the physical, mechanical, and durability characteristics of concrete. Buildings 2024;14(4):1148. https://doi.org/10.3390/buildings14041148
40. Gursel, A. P., Masanet, E., Horvath, A., & Stadel, A. (2014). Life-cycle inventory analysis of concrete production: A critical review. *Cement and Concrete Composites, 51*, 38-48. **https://doi.org/10.1016/j.cemconcomp.2014.02.004**
41. S. Yagi, C. Aquino, M. Inoue, & T. Okamoto, "Volume change of limestone and its effects on drying shrinkage of concrete", Advanced Materials Research, vol. 168-170, p. 738-741, 2010. https://doi.org/10.4028/www.scientific.net/amr.168-170.738
42. R. Mu, W. Tian, & Y. Guo, "Effect of aggregate on drying shrinkage of concrete", Advanced Materials Research, vol. 168-170, p. 701-708, 2010. https://doi.org/10.4028/www.scientific.net/amr.168-170.701
43. W. Shen, Z. Yang, Z. Yang, J. Li, L. Cao, & C. Zhang, "Scattering-filling stone concrete: mechanism, experiment and utilization", Key Engineering Materials, vol. 629-630, p. 522-527, 2014. https://doi.org/10.4028/www.scientific.net/kem.629-630.522
44. L. Hua, J. Aguiar, X. Wan, Y. Wang, S. Cunha, & Z. Jia, "Application of aggregates from construction and demolition wastes in concrete: review", Sustainability, vol. 16, no. 10, p. 4277, 2024. https://doi.org/10.3390/su16104277
45. X. Chen, Y. Shi, Y. Lin, X. Li, S. Zhou, & K. Xiao, "Influence of aggregates on cracking sensitivity of concrete", Applied Mechanics and Materials, vol. 368-370, p. 939-944, 2013. https://doi.org/10.4028/www.scientific.net/amm.368-370.939
46. I. Maruyama and A. Sugie, "Numerical study on drying shrinkage of concrete affected by aggregate size", Journal of Advanced Concrete Technology, vol. 12, no. 8, p. 279-288, 2014. https://doi.org/10.3151/jact.12.279

47. L. Rendón, M. Rendon, & N. Ramirez, "Lwa as internal curing agent to control availability of internal curing water in concrete", Mrs Proceedings, vol. 1612, 2013. https://doi.org/10.1557/opl.2013.1125
48. M. Karagüler and M. Yatağan, "Effect of aggregate size on the restrained shrinkage of the concrete and mortar", Moj Civil Engineering, vol. 4, no. 1, p. 15-21, 2018. https://doi.org/10.15406/mojce.2018.04.00092
49. W. Zhang, M. Zakaria, & Y. Hama, "Influence of aggregate materials characteristics on the drying shrinkage properties of mortar and concrete", Construction and Building Materials, vol. 49, p. 500-510, 2013. https://doi.org/10.1016/j.conbuildmat.2013.08.069
50. F. Soomro, B. Memon, M. Oad, A. Buller, & Z. Tunio, "Shrinkage of concrete panels made with recyclable concrete aggregates", Engineering Technology & Applied Science Research, vol. 9, no. 2, p. 4027-4029, 2019. https://doi.org/10.48084/etasr.2595
51. J. Jeong, Y. Park, & Y. Lee, "Variation of shrinkage strain within the depth of concrete beams", Materials, vol. 8, no. 11, p. 7780-7794, 2015. https://doi.org/10.3390/ma8115421
52. P. Ng and A. Kwan, "Strategies for improving dimensional stability of concrete", Canadian Journal of Civil Engineering, vol. 43, no. 10, p. 875-885, 2016. https://doi.org/10.1139/cjce-2016-0090

Transportation Infrastructure Durability Center
AT THE UNIVERSITY OF MAINE

35 Flagstaff Road
Orono, Maine 04469
tidc@maine.edu
207.581.4376

www.tidc-utc.org